

A Gastight Microfluidic System Combined
with Optical Tweezers and Optical Spectroscopy
for Electrophysiological Investigations
of Single Biological Cells

Ahmed Alrifaiy

A gastight microfluidic system combined with optical tweezers and optical spectroscopy for electrophysiological investigations of single biological cells

Ahmed Alrifaiy

Dept. of Computer Science, Electrical and Space Engineering
Luleå University of Technology
Luleå, Sweden

Supervisors:

Kerstin Ramser and Olof Lindahl

Printed by Universitetsstryckeriet, Luleå 2011

ISSN: 1402-1757
ISBN 978-91-7439-351-4

Luleå 2011

www.ltu.se

To my father

ABSTRACT

Stroke affects around 20 million people around the world every year. Clinically, stroke is a result of brain damage due to the shortage of oxygen delivered to the nerve cells. To minimize suffering and costs related to the disease, extensive research is performed on different levels. The focus of our research is to achieve fundamental understanding on how the lack of oxygen in brain tissue activates intrinsic biomolecular defense mechanisms that may reduce brain damage. More knowledge may hopefully lead to new therapeutic and preventive strategies on the molecular level for individuals in the risk zone for stroke or those who have just suffered a stroke.

The area of study is based on the discovery of a hemoprotein called neuroglobin (Ngb), which is found in various regions in the brain, in the islets of Langerhans, and in the retina. Several studies have shown that Ngb seems to have a protective function against hypoxia-related damage. However, until now, it has not been understood how Ngb affects the nerve system and protects neurons from damage.

The well-established patch-clamp technique is routinely used to measure and analyze the electrophysiological activity of individual biological cells. To perform accurate patch-clamp experiments, it is important to create well-controlled physiological conditions, i.e. different oxygen levels and fast changes of nutrients and other biochemical substances. A promising approach is to apply lab-on-a-chip technologies combined with optical manipulation techniques. These give optimal control over fast changing environmental conditions and enable multiple readouts.

The conventional open patch-clamp configuration cannot provide adequate control of the oxygen content. Therefore, it was substituted by a gas-tight multifunctional microfluidic system, a lab-on-a-chip, with an integrated patch-clamp micropipette. The system was combined with optical tweezers and optical spectroscopy. Laser tweezers were used to optically guide and steer single cells towards the fixed micropipette. Optical spectroscopy was used to investigate the biochemical composition of the sample. The designed, closed lab-on-a-chip acted as a multifunctional system for simultaneous electrophysiological and spectroscopic experiments with good control over the oxygen content in the liquid perfusing the cells.

The system was tested in a series of experiments: optically trapped human red blood cells were steered to the fixed patch-clamp pipette within the microfluidic system. The oxygen content within the microfluidic channels was measured to 1 % compared to the usual 4-7 %. The trapping dynamics were monitored in real-time while the spectroscopic measurements were performed simultaneously to acquire absorption spectra of the trapped cell under varying environments. To measure the effect of the optical tweezers on

the sample, neurons from rats in a Petri dish were optically trapped and steered towards the patch-clamp micropipette where electrophysiological investigations were performed. The optical tweezers had no effect on the electrophysiological measurements. Similar investigations within a closed microfluidic system were initiated and showed promising results for further developments of a complete lab-on-a-chip multifunctional system for reliable patch-clamp measurements.

The future aim is to perform complete protocols of patch-clamp electrophysiological investigations while simultaneously monitoring the biochemical composition of the sample by optical spectroscopy. The straightforwardness and stability of the microfluidic chip have shown excellent potential to enable high volume production of scalable microchips for various biomedical applications. The subsequent ambition is to use this system as a mini laboratory that has benefits in cell sorting, patch-clamp, and fertilization experiments where the gaseous and the biochemical content is of importance. The long-term goal is to study the response of individual neurons and defense mechanisms under hypoxic conditions that may establish new ways to understand cell behavior related to Ngb for various diseases such as stroke, Alzheimer's and Parkinson's.

CONTENTS

Part I	1
CHAPTER 1 – LIST OF PUBLICATIONS AND MY CONTRIBUTIONS	3
1.1 The publications included in the licentiate thesis	3
1.2 Other publications not included in the licentiate thesis	4
CHAPTER 2 – INTRODUCTION	5
2.1 General background	5
2.2 The aim of the research	8
CHAPTER 3 – ABBREVIATIONS	9
CHAPTER 4 – THEORY	11
4.1 Patch-clamp technique	11
4.2 Optical tweezers	12
4.3 Microfluidic system	18
4.4 Optical spectroscopy	23
CHAPTER 5 – METHODS AND MATERIALS	27
5.1 Experimental setup	27
CHAPTER 6 – RESULTS AND DISCUSSIONS	33
6.1 Results and discussions	33
CHAPTER 7 – CONCLUSIONS	37
CHAPTER 8 – FUTURE OUTLOOK	39
CHAPTER 9 – REFERENCES	41
 Part II	 51
PAPER A	53
PAPER B	55
PAPER C	57

ACKNOWLEDGMENTS

I would like to thank all those who gave me the possibility to complete this licentiate work. First of all, I would like to express my gratitude to my supervisor, Kerstin Ramser, for guidance, stimulating suggestions, support and encouragement during my research, which has enabled me to develop an understanding for the subject.

Special thanks go to my co-supervisor, Olof Lindahl, for the guidance and support during my research and writing of my licentiate work. I would like to thank my colleagues at the Division of Biomedical Engineering , especially Nazanin Bitaraf for the valuable contribution and cooperation in the project, Stefan Candefjord and Morgan Nyberg.

I am obliged to my colleagues at the Department of Computer Science, Electrical and Space Engineering , especially to Johan Borg and Mikael Larsson, for valuable inputs and helpful suggestions for improvement of the experimental work. I am very grateful to my project partners at Umeå university, section of physiology, especially Staffan Johansson, Michael Druzin and Evgenya Malinina for excellent and worthwhile cooperation during the project. To my family, I would like to give my special thanks for patience and support.

Finally, I would like to thank EU Structural fund, Objective 2, Norra Norrland, the Swedish Research Council, and the Kempe Foundation for supporting this work.

Part I

CHAPTER 1

List of publications and my contributions

1.1 The publications included in the licentiate thesis.

(A) A. Alrifaiy, N. Bitaraf, O. Lindahl and K. Ramser, "Development of microfluidic system and optical tweezers for electrophysiological investigations of an individual cell", Proceedings of SPIE, the International Society for Optical Engineering, vol. 7762, 77622k1-77622k7, 2010.

(B) A. Alrifaiy and K. Ramser, "How to integrate a micropipette into a closed microfluidic system: Absorption spectra of an optically trapped erythrocyte," OSA, Biomedical optics express 2 (8), 2299-2306 2011.

(C) A. Alrifaiy, N. Bitaraf, O. Lindahl and K. Ramser, "Hypoxia on a chip - a novel approach for patch-clamp in a microfluidic system with full oxygen control", submitted to 12th World Congress on Medical Physics and Biomedical Engineering, Beijing, China, 2012.

1.1.1 My contributions

My contributions to paper A, B and C. 1 = mainresponsibility, 2 = Contributed to high extent, 3 = Contributed.

Parts	Paper A	Paper B	Paper C
Idea and formulation of the Study	2	1	2
Experimental design	1	1	2
Performance of the experiments	1	1	2
Analysis of results	1	2	2
Writing of manuscript	2	2	2

1.2 Other publications not included in the licentiate thesis

(I) N. Bitaraf, A. Alrifaiy, M. Druzin, and K. Ramser, "Development of a multifunctional microfluidic system for studies of nerve cell activity during hypoxic and anoxic conditions", 11th World Congress on Medical Physics and Biomedical Engineering, , Munich, Germany, Springer Science+Business Media 8, 176-179, 2009.

(II) N. Bitaraf, K. Ramser and A. Alrifaiy", "Multipla mätningar på enstaka celler i ett mikroflödessystem", Medicinteknikdagarna i Västerås, Conference abstract, Västerås, Sweden, 2009.

(III) A. Alrifaiy, O. Lindahl, and K. Ramser, "Ett mikroflödessystem med optisk pincett och UV- vis för studier på enskilda biologiska celler", Medicinteknikdagarna i Umeå, Conference abstract, Umeå, Sweden, 2010.

(IV) A. Alrifaiy, N. Bitaraf, O. Lindahl and K. Ramser " Ett mikroflödessystem för multipla undersökningar av enstaka biologiska celler under hypoxiska förhållande", Medicinteknikdagarna i Linköping, Conference abstract, Linköping, Sweden, 2011.

CHAPTER 2

Introduction

2.1 General background

2.1.1 Stroke

Stroke is the second most common cause of death and disability in the world [1], and it affects people of all ages -including children. Statistically, the risk of stroke increases for people older than 60 years. Higher risks for stroke are associated with high blood pressure (hypertension), heart disease, and diabetes. Ischemic stroke covers about 88% of all strokes and occurs due to a rapid loss of brain function(s) caused by disturbance of the blood supply to the brain.

The main function of the blood flow is to supply oxygen and nutrients to the tissue and to transport carbon dioxide and cellular waste out of the body. An interruption of the blood flow and the oxygen delivery to the neural system and the brain affects the function of the individual cells. The consequences are death or disability due to brain damages [2].

Physiologically, ischemic strokes [3] are classified as thrombotic or embolic. A thrombotic stroke (cerebral thrombosis or infarction) occurs when blood clots are formed that block the arteries in the brain. This kind accounts for 50% of all ischemic strokes. Large-vessel thrombosis is a blockage in one of the brain's larger blood-supplying arteries such as the carotid or middle cerebral arteries. Small-vessel thrombosis (lacuner stroke) is the blockage of one or more of the smaller arteries that penetrate deeply into the brain. An embolic stroke occurs when a blood clot (embolus) forms within an artery that is usually outside of the brain, e.g., in the heart. The clot travels with the blood flow until it becomes lodged. Both types of stroke restrict the natural flow of blood to the brain and result in immediate physical and neurological deficits. Many studies have investigated the cause, prevention, immediate treatment after a stroke, and the long-term rehabilitation after a stroke [4].

2.1.2 Hemoproteins

Hemoprotein (or hemoglobin, Hb), in red blood cells, serves as the oxygen carrier in blood [5]. The presence of hemoglobin in blood increases the oxygen-carrying ability and the transport of carbon dioxide from the tissues back to the lungs.

The name hemoglobin comes from heme and globin, since each subunit of hemoglobin is a globular protein with an embedded heme group. Each heme group contains an iron atom, which is responsible for the binding of oxygen. During breathing, O_2 in airsacs (alveoli) of the lungs passes through the thin-walled alveolar walls, the thin-walled blood vessels, and enters into the red blood cells, where it binds to the hemoglobin (oxy-hemoglobin). The blood is then circulated around the body until it reaches tissues and cells that are rich in CO_2 , a waste product of cellular processes. The CO_2 displaces the weakly-bound O_2 and forms carbaminohemoglobin, which then travels in the blood back to the lungs where it is again displaced by oxygen [6].

In 2000, a new oxygen-binding hemoprotein called neuroglobin (Ngb) [7] was identified. It is mainly found in neurons, in the islets of Langerhans, and in the retina [8]. The abundance, localization and 3D chemical structure of the protein have been studied and determined [9-13]. However, the exact function of the protein is still uncertain [14]. A protective role of Ngb against hypoxic or ischemic injury has been shown [15], and neuronal hypoxia induces Ngb expression and reduces hypoxic neuronal injury [16]. While previous research mainly has focused on investigations of the protein in its purified form, the challenge is to investigate the mechanism of action of Ngb in a functioning biological cell during oxygen deprivation.

2.1.3 Electrophysiological investigations under environmental control

Investigations of functional living nerve cells should be carried out under well-controlled physiological conditions, i.e. under different oxygen levels and during the addition/removal of biochemical substances or nutrients. One method that routinely used is the patch-clamp technique that measures the electrophysiological signaling of nerve cells. The major technical challenge with the patch-clamp technique is steering the cells to the recording sites, successfully forming gigaohm seals to measure pA currents, and achieving low-noise recordings. It would be desirable to introduce new patch-clamp approaches to render experiments less challenging and to enhance the throughput. However, to introduce new systems successfully, the new techniques need to be compared and verified with traditional patch-clamp configurations [17].

In some studies, planar patch-clamp investigations [18] have been performed by integrating the traditional patch-clamp technique with "lab-on-a-chip" technologies. The patch-clamp micropipette with a conic tip is obtained by a planar micropipette (conic holes in a silicon-based microfluidic system). The technique was introduced to improve the noise performance by using low-loss dielectric materials and to achieve cost effectiveness and high throughput screening [19].

The field of cell biology microfluidics has become an essential tool for analysis of living

cells. Microfluidics have many unique features. The methods use minimal amounts of reagents and analytes, they can function as portable clinical diagnostic devices, and can thus reduce expensive and time-consuming laboratory analysis procedures. The significant benefits are the control of cell transport, immobilization, manipulation of biological molecules and cells, and mixing of chemical reagents [20-21]. This enables advanced analysis of intracellular investigations on the single-cell level in an environment-controlled analytical system [22-23].

Microfluidic systems, also referred to as "lab-on-a-chip" or μ TAS (Micro Total Analysis Systems), typically consist of micro-sized channels of 10-1000 μ m diameter, which allow for fluid flow rates down to a few pl/s . They are usually made of materials such as PDMS (Poly-DiMethyl Siloxane), PMMA (Poly-Methyl MethAcrylate), or glass for optical transparency and the ease of implementation onto microscopes in combination with suitable read-out techniques.

Nowadays, PMMA microchips have become popular in various biological and medical applications [24]. They are less expensive than glass microchips [25] and simple to fabricate compared to lithographical microchips [26]. The main advantage of using PMMA is the impermeability to air, gases and other important properties like low toxicity, optical transparency, thermal stability and easy manufacturing [27]. The use of PMMA-based devices has been shown useful in many situations, e.g. for micro-mixers [28], polymerase chain reaction microchips (PCR) [29], microfluidic reactors [30] and capillary electrophoresis microchips (CE) [31].

Investigations of biological cells are carried out on microscopes often combined with various optical techniques such as optical spectroscopy or time-resolved techniques. Recently, much attention has been paid to setups combined with optical tweezers [32] and microfluidic systems [33]. These setups have enabled innovative approaches for basic and applied research for diverse biological studies of single cells [34].

Optical tweezers have emerged as important tools in biophysics and cell biology. They utilize light to trap and manipulate small particles in three dimensions. Stable optical traps are formed by a strongly focused laser beam. The phenomenon of using light radiation to manipulate small objects was experimentally demonstrated on atoms [35] and later for manipulation of biological cells using near infrared lasers [36]. The applications of optical tweezers are found in many research areas such as cell transport and separation [37], manipulation of biological cells [38], sample cell analysis by mass spectrometry [39], DNA analysis [40] and other applications for clinical diagnostics [41].

Combinations of microfluidic systems with optical manipulation techniques have shown a great impact on the ongoing revolution in cell biology and biotechnology [42-43]. As a result, several studies relating to single cell manipulation in environment-controlled microfluidic systems for biological cell analysis have been published during the past few years [44-46]. Consequently, it is also valuable to apply this system for advanced electrophysiological investigations of single biological objects with precise environmental control.

The main goal of our research is to investigate the functional role of neuroglobin (Ngb) *in vivo*, i.e., on living biological cells under hypoxic and anoxic conditions [47-48] in order

to learn more about the ability of Ngb to affect the electrophysiological signaling capacity of nerve cells during fast environmental changes. The long-term aim is to clarify the mechanism of the protective role of Ngb. As shown in this thesis, the traditional patch-clamp technique was used to perform accurate electrophysiological studies on individual neurons. However, it was difficult to acquire measurements under well-controlled oxygen levels since the cells were kept in an open environment exposed to ambient oxygen. The idea is to modify the patch-clamp technique to enable electrophysiological measurements on a single cell, by using a closed microfluidic system combined with optical tweezers and optical spectroscopy.

The main goal was to enable electrophysiological measurements on single cells during well-controlled environmental conditions, i.e. different oxygen levels. An investigated single cell was trapped and steered by optical tweezers through the microfluidic channel-system towards the fixed micropipette. The electrophysiological investigations were then performed while exposing the investigated cell to solutions with varied oxygen level. Simultaneously, optical UV-Vis spectroscopy was used to study the biochemical composition of the investigated cell in real-time.

2.2 The aim of the research

The aim of this licentiate work was to develop experimental tools to reproduce hypoxia on a chip. The particular aims were:

(A) To design a first model of a closed microchip with an integrated patch-clamp micropipette that enables enhanced control over the environment. This aim included integration of optical tweezers to steer single cells within the microfluidic channels to establish contact with the integrated patch-clamp pipette. Furthermore, the aim also included to simultaneously monitor the real-time trapping dynamics and acquiring spectroscopic absorption spectra of the trapped cell under variations in the environment.

(B) To design a new prototype of a PMMA-based closed microfluidic system for electrophysiological investigations with reliable control over the environment i.e. to integrate a patch-clamp micropipette within the microfluidic channels so that the optically trapped cell could be attached to the micropipette.

(C) To improve the closed microfluidic chip for electrophysiological patch-clamp investigations combined with optical tweezers.

CHAPTER 3

Abbreviations

CCD	Charge-Coupled Device
CNC	Computer Numerical Control
ECS	ExtraCellular Solution
GMM	Gimbal Mounted Mirror
IC	Integrated Circuit
ICS	IntraCellular Solution
NA	Numeric Aperture
Re	Reynolds number
RBC	Red Blood Cell
PBS	Phosphate-Buffered Saline
PDMS	Poly-DiMethyl Siloxane
PMMA	Poly-Methyl MethAcrylate
TEM00	Transverse Electromagnetic Mode-lowest order
UV-Vis	Ultraviolet-visible
μ TAS	Micro Total Analysis Systems
SLM	Spatial Light Modulator

CHAPTER 4

Theory

The chapter will provide basic theories behind methods and materials used in my experimental work.

4.1 Patch-clamp technique

Patch-clamp [49] is a well-established method used in the field of physiology and other medical applications. The technique allows for measurements of the electrophysiological activity of individual biological cells under variable surroundings by recording tiny electrical signals across the ion channels in the plasma membrane of the cell [50]. The setup consists mainly of a solution-filled glass micropipette with a tip of 1-5 μm in diameter. The pipette is manipulated in three dimensions by an electronically steered micro precision tool to attach to the membrane of a single cell or a cell in a tissue slice located in the open Petri-dish. To register electrophysiological signals, a gigaohm resistance seal, obtained by applying negative pressure (i.e, sucking), [51] is required between the cell membrane and the pipette. The signals are registered through a recording electrode inside the patch-clamp pipette and a reference electrode in contact with the cell's immediate environment, which is experimentally changed by perfusion of different solutions, see Figure 4.1.

The observable limitation of patch-clamp is the sensitivity that requires an alert design of electronics and apparatus to allow for low-noise recordings and precise positioning of the pipette towards the cell. Positive outcome of experiments mainly depends on the experience and patience of the researcher. The setup's sensitivity requires that it is placed inside of a Faraday cage to block out external static and non-static electric fields. The sensitivity of the technique limits the possibility to exploit all information from one cell during an investigation and has low experimental throughput, i.e., few cells measured per day by one operator, [52].

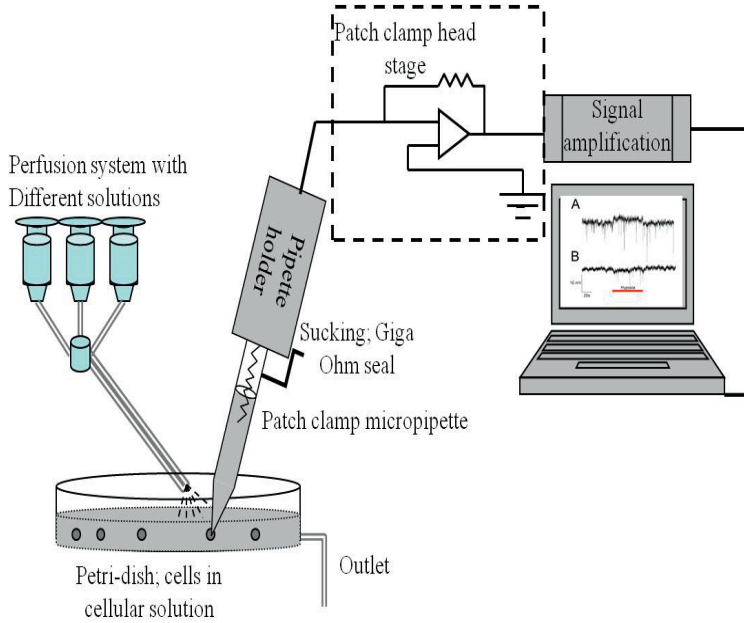


Figure 4.1: A schematic setup of a traditional patch-clamp configuration including a micropipette mounted on a pipette holder on a head stage, a signal amplifier, a perfusion system and a computer with a software program for signal analysis and recording

4.2 Optical tweezers

The theory behind the optical tweezers [53] is based on the transfer of momentum between light radiation and a dielectric particle due to refraction or scattering of light. Newton's 2nd law of momentum conservation states that the transfer of momentum from the light to the refracting particle suspended in media of lower refractive index gives rise to forces acting on the particle in three dimensions.

The phenomenon of optical trapping is generated from three-dimensional steep gradients from a laser beam which is focused to a diffraction-limited spot in the specimen plane of a microscope. Thus, small dielectric objects, such as biological cells, found in the focus of light, will experience radiation pressure forces. A gradient force pushes the cell towards the central region with the highest intensity of the Gaussian beam, and a scattering force pushes the cell in the direction of the light. Stable optical trapping occurs when the gradient force is sufficiently large to overcome the scattering force [54].

In general, the steepest gradients in light are obtained by focusing a laser beam through a high numerical aperture microscope objective. The numerical aperture (NA) is defined as the ratio of the indices of refraction of the particle and the surrounding media (air, water, or oil) multiplied by the sine of the half-angle of opening of the

focused light, $NA = \frac{n_p}{n_m} \sin \alpha$ [55]. A typical value for a high-NA objective is 1.00-1.40 when $n_p > n_m$ and the full angle of opening is about 140° [56]. The theoretical approach of the trapping forces is generally represented by two configurations related to the size of the trapped particle. Raleigh theory is valid when the trapping wavelength is greater than the diameter of the trapped object $\lambda > d$, while Mie theory is valid when $\lambda < d$ [57]. Most biological cells are of sizes fitted between Mie and Raleigh regimes, where the trapping forces are estimated numerically.

4.2.1 Raleigh theory

The trapped object is illustrated as a dielectric dipole in a non-homogeneous electromagnetic field [58]. The gradient force is induced by the gradient in the electromagnetic field and related proportionally to the gradient of intensity of the light. The three-dimensional gradient force is directed towards the center of the higher intensity and is defined as:

$$F_g = -\frac{r^3 n_m^3}{2} \left(\frac{m^2 - 1}{m^2 + 2} \right) \nabla E^2 \quad (4.1)$$

The scattering force F_{sc} for the dielectric dipole in the electric field is given by:

$$F_{sc} = \frac{128\pi^5 r^6 n_m}{3c\lambda^4} \left(\frac{m^2 - 1}{m^2 + 2} \right)^2 I \quad (4.2)$$

Where, c is the velocity of light, λ is the wavelength of light, r is the radius of the particle, $m = n_p/n_m$ is the effective index of refraction for the particle n_p to the medium n_m and I is the intensity of the light. Eq1. and Eq2. show clearly that the forces F_g and F_{sc} are both proportional to the radius of the particle and to the intensity of the light.

4.2.2 Mie theory

The theory makes use of ray optics configuration to explain the optical forces acting on a particle represented by a spherical bead [57]. The rays of light with various intensities are symbolized by straight lines and follow Snell's law of refraction and Fresnel's equations for reflection and transmission. The scattering and gradient forces for a single ray in Mie regime are calculated as:

$$F_{sc} = p \frac{n_m}{c} \left(1 + R \cos 2\beta - T^2 \left(\frac{\cos(2\beta - 2\alpha) + R \cos 2\beta}{1 + R^2 + 2R \cos 2\alpha} \right) \right) \quad (4.3)$$

$$F_g = p \frac{n_m}{c} \left(R \sin 2\beta - T^2 \left(\frac{\cos(2\beta - 2\alpha) + R \cos 2\beta}{1 + R^2 + 2R \sin 2\alpha} \right) \right) \quad (4.4)$$

Where R and T are the Fresnel coefficients for reflection and transmission, β and α are the angles of the incident and reflected, and $P \cdot \frac{n_m}{c}$ is the momentum transferred by the ray. The total forces by a beam on the particle are the contributions of all rays using Eq3. and Eq4. by numerical integration over all angles [59].

4.2.3 Experimental considerations

The trapping of particles in three spatial dimensions requires a sufficiently steep intensity gradient of light in both the lateral (x-y plane) and axial (z) directions [60]. The force components acting on the trapped particle are shown in Figure 4.2, where the axial and lateral trapping have been separated for simplicity.

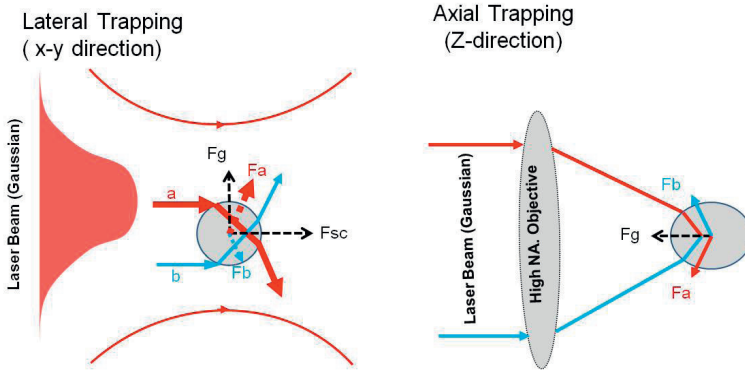


Figure 4.2: Axial and lateral trapping of a dielectric particle in a Gaussian laser beam, trapped in laser light focused by a high numerical aperture objective. A) Axial trapping arises through the compensation of the scattering force (which pushes the bead in the direction of beam propagation) by the gradient force (which acts towards the focal spot). B) Lateral trapping arises from the gradient force, which acts towards the higher intensity region of the Gaussian beam profile.

The interaction of the dielectric particle with laser light will produce net lateral forces acting towards the high intensity region of the beam. The intensity gradient in the x-y

plane pushes the particle to the center (trapping in the x-y direction) due to the symmetry of the Gaussian laser beam. The scattering force component from the radiation pressure pushes the particle in the direction of laser beam propagation (z-direction). For complete 3-D trapping, the scattering force must be canceled out by a force induced by the steep intensity gradient in the z-direction, towards the focal point of the objective and opposite to the scattering force. Figure 1 shows the two rays, F_a (represents the more intense ray) and F_b , in the directions of propagation that result in a scattering force F_{sc} pushing the particle away from the laser. F_g represents the force due to the larger gradient in the F_b direction, which results in movement of the particle towards the center of the beam. The axial trapping in the direction of propagation of the focused beam arises due to the gradient forces, F_a and F_b , which result in a force, F_g , in the direction opposite the direction of the force F_{sc} .

4.2.4 Basic design of optical tweezers

Figure 4.3 shows the basic design of a functional optical trap in the specimen (x-y) plane and in the axial (z-) direction, which can be adapted to work with most inverted research microscopes. By additional modifications, the setup can be used with other imaging modes such as bright-field, dark-field, phase contrast, and differential interference contrast [61].

The setup is preferably built on an inverted microscope mounted on a vibration-free optical table with optional controlled conditions of temperature, noise and air turbulences. The system includes a trapping laser, a beam expander, optical lenses and mirrors to steer the beam position in the sample plane, and optionally a position detector (such as a quadrant photodiode) to measure beam displacements and trap stiffness. The microscope is equipped with a port for introducing the trapping laser, a CCD camera for high-resolution video and image recordings and position monitoring of the trapped object, an illumination source, a high numerical aperture (NA) microscope objective, and a condenser to generate the optical trap in the sample plane.

In practice, the trapping lasers are in the lowest-order mode TEM_{00} , or they are single mode diode lasers to achieve the steepest light gradient [62]. The laser power varies from 10 mW to 1 W. Typically, lasers of 785-1064 nm are widely used for trapping due to the low absorption coefficient of the aqueous solution at these wavelengths that minimizes the effect of heating or damaging the samples [63]. The high-NA objective is essential to obtain the stable trap by generating a gradient force that is greater than the scattering force.

The alignment of optical tweezers starts, according to Figure 4.3, by directing the laser beam through mirror M_1 to the beam expander. The two lenses, L_1 and L_2 , have suitable focal lengths to obtain a magnified parallel beam filling the back aperture of the objective to obtain a tight diffraction-limited spot [64]. The beam is then guided by another mirror, M_2 , mounted on an xyz translation stage or GMM (gimbal mounted mirrors) through a beam-steering system into the microscope. The laser beam is steered through a dichroic mirror and a microscope objective to the sample plane. The visualization of the trapping

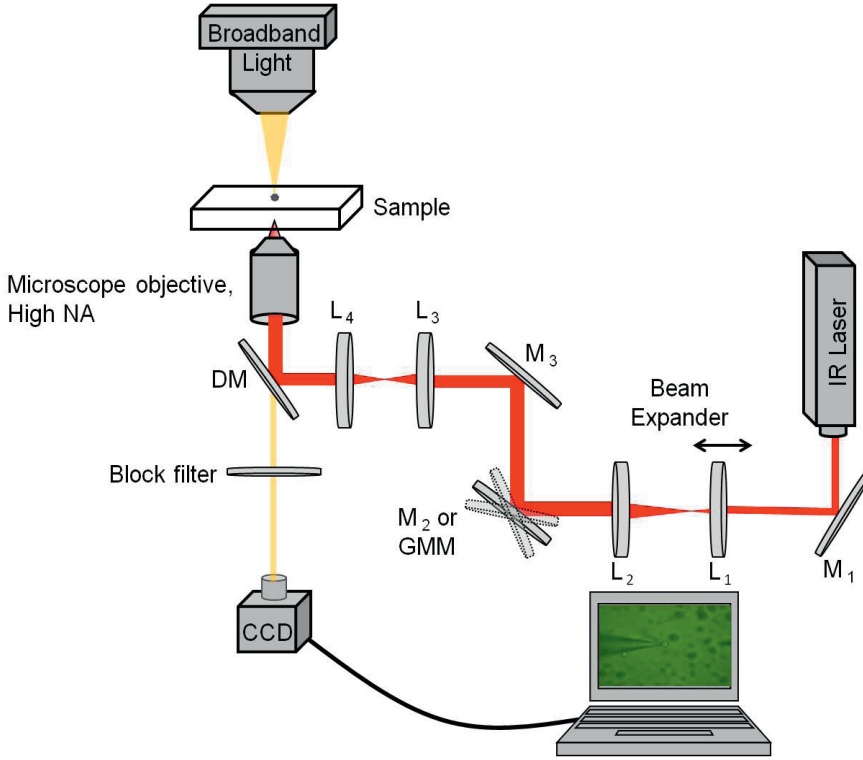


Figure 4.3: A schematic design of optical tweezers build on an inverted microscope with CCD imaging camera, including laser, beam expander, L_1 and L_2 , beam steering, L_3 and L_4 , dichroic mirror, DM, steering mirrors, M_1 , M_2 and M_3 , and a high-NA microscope objective.

dynamics on the sample plane is usually accomplished through a microscope light source that passes the optical path in the direction opposite to the direction of the trapping laser. The light source is then transmitted through the dichroic mirror and reaches a CCD camera protected by a laser block filter and connected to an external monitor. The 3-D position of the trapped particle is usually controlled either by adjusting the focal point and angle of the input beam or by moving the sample.

4.2.5 Laser beam steering

Beam steering of the laser spot, shown in Figure 4.4 and 4.5, is simply performed by the two identical planoconvex lenses, L_3 and L_4 , placed at a distance equal to the sum of their focal lengths. L_4 is mounted on the xyz translation stage, or micromanipulator, i.e. the movement of this lens in three dimensions corresponds to the movement of the laser trap in the same three dimensions. As shown in Figure 4.4, the axial direction of

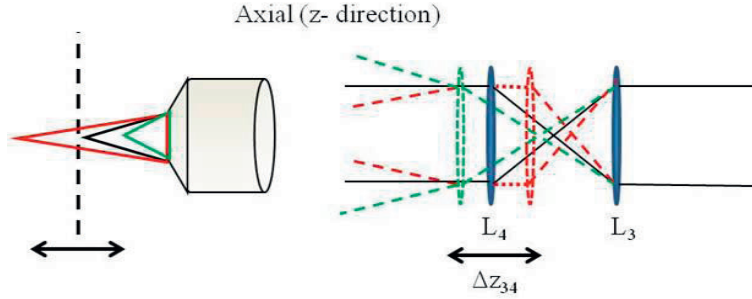


Figure 4.4: Axial trapping obtained by axial translation of lens L_4 in the beam steering.

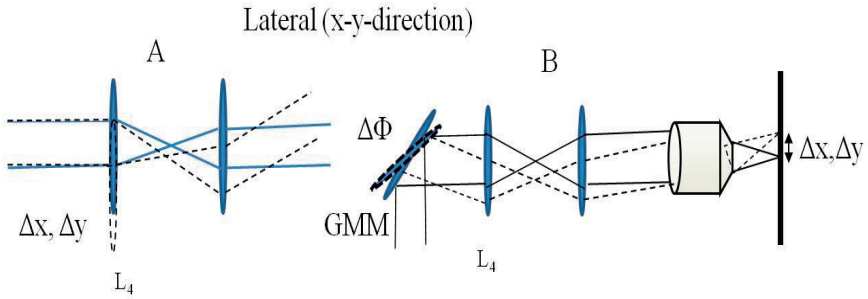


Figure 4.5: A schematic design of optical tweezers build on an inverted microscope with CCD imaging camera, including laser, beam expander, L_1 and L_2 , beam steering, L_3 and L_4 , dichroic mirror, DM, steering mirrors, M_1 , M_2 and M_3 , and a high-NA microscope objective.

the trap is easily controlled by changing the divergence or the convergence of the laser beam by moving L_4 where small displacements, Δd_{34} , between L_3 and L_4 , result in the corresponding axial displacement of the focus Δz [65]. The lateral translation of the trap relative to the sample is, in many designs, accomplished by the translation of the microscope stage. However, it is valuable to use a beam-steering system for an extra degree of translational freedom. As shown in Figure 4.5A and 4.5B, the translation of the lens L_4 in the lateral plane (x-y plane), perpendicular to the optical axis, provides a lateral deflection of the laser beam that result in a proportional lateral translation in the sample plane. In some designs, gimbal mounted mirrors (GMM) are used to perform the lateral translation by moving the laser beam instead of moving L_4 in the x-y plane, as shown in Figure 4.5B.

4.2.6 Applications for optical tweezers

The main application for optical trapping techniques is the manipulation of microscopic objects and the sensitive estimation of trapping forces. The optical tweezers have been widely used for biological cell sorting [66], active modification of polymer structures (DNA melting, membrane deformation strength and separating of protein polymers), characterization of molecular motors such as myosin and kinesin, and for accurate measurements of binding forces in the biological and medical fields [67-73]. In addition, in vitro optical manipulation, as a sterile method, causes less growth inhibition of biological cells [32,74-75]. For pathological application, Optical tweezers are widely used as contact-free micro dissection tools, so called "laser scalpels" [76]. The technique is considered as an inexpensive tool for various applications due to the easy intergradations with most commercial microscopes.

4.3 Microfluidic system

The field deals with designs of microfluidic devices to enable precise control of the fluid flow through micro-sized channels connected by reservoirs or sealed inlets and outlets.

4.3.1 Characterization of the fluid flow

The behavior of the fluid flow in most microfluidic applications is expressed as laminar or turbulent flow. The laminar flow, also called streamline flow, indicates that the fluidic properties such as velocity and pressure are time-independent at each point within the fluid. Thus, the fluid flow behaves smoothly in regular paths under constant boundary conditions [77] with convective mass transfer in the direction of the flow. The fluid flow in microchannels is characterized by the Reynolds number (Re), which describes the tendency of fluids to develop turbulence. A quantitative estimation of (Re) is represented by the ratio of inertial and viscous forces on the fluid [78]:

$$Re = D_h \cdot \frac{\nu}{\mu} \quad (4.5)$$

Where μ is the kinematic fluidic viscosity, ν is the average velocity of the fluid, and D_h is the hydraulic diameter, a characteristic number of the volume-to-area ratio of the channel [79]. The laminar flow is achieved by designing small microfluidic channels with slow fluid flow and relatively high viscosity. The phenomenon is distinguished by the laminar flow of the blood through capillaries in the human body [80]. For $Re > 2000$, the fluid flow experiences turbulent behavior where the fluid undergoes irregular fluctuations and mixing, and the convective mass transport takes place in all directions [33,81]. Since the length of microfluidic channels is small, typically $< 500 \mu\text{m}$, the Reynolds number is low, e.g. typically $Re < 10$, and the fluid flow is laminar. The liquids behave as laminae

(layers) of uniform thickness moving between fixed boundaries, and the only mixing of the streams occurs by diffusion across the liquid-liquid interfaces [82].

4.3.2 The fluid transport

The most critical issue is to optimize the fluid flow within the microfluidic channels. Experimentally, the flow can be generated from high volume rates used for cytometry [83-84] to low rates of pl/s in applications demanding nano- and micro-scaled channels [85]. In some applications, the fluid transport can be controlled by the fluidic mass transport due to diffusion [86]. This can be explained by the thermal energy when particles spread in the fluid due to the Brownian motion. In most applications, the control of the fluid transport is achieved by using external pump systems. The pump systems are chosen depending on the range of quantities transported, the behavior of the transported fluid and mainly the influence on the measurements. The main methods in fluid transport are pressure-driven flow [87], electro-osmotic flow [88] and fluid transport by using motor proteins [89].

Pressure-driven flow

This common method uses either embedded micro-pumps within the microfluidic chip, or external pump systems to generate external pressure flow such as the positive displacement pumping [90] and the ultra-precise syringe pump systems [88]. The advantage is the capability to control the exact amount and location of the pumped fluid. The limitations are the difficulty to achieve smooth fluid flows at very low rates within small channels and the non-uniform velocity profile of the flow [77] as shown in Figure 4.6. The pseudo-parabolic profile shows that the maximal velocity of the fluid is in the center of the channel, which decreases to zero on the walls. The phenomenon can be investigated by software simulations using Navier Stokes equations with proper boundary conditions [91].

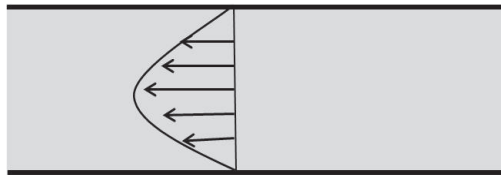


Figure 4.6: The fluid flow profile within the microfluidic channels, A) pseudo-parabolic profile in pressure-driven flow, B) a uniform velocity profile in electro-osmotic driven flow.

4.3.3 The fabrication of microfluidic devices

Microfluidic devices were initially fabricated from non-polymeric materials such as silicon or glass, using the well established integrated circuit (IC) production techniques. The most common techniques are photolithography and surface micro-matching, mostly due to the equipment availability and the possibility to integrate microfluidics with electronics.

While fabrication techniques for silicon and glass microfluidic devices are well established, the present research and commercialization has shifted the focus to micro devices made completely from polymeric materials. The main benefits are low cost, durability, and the availability of many mechanical and chemical properties achievable based on simple chemical changes in the polymer formulations. Since each device requires considerable resources to develop and produce, efforts have been made to reduce the optimization time through the use of rapid prototyping techniques, where device geometries are quickly evaluated [92]. Until now, the most promising techniques for fabrication of polymeric micro devices have utilized silicon rubber (Poly-DiMethyl Siloxane, PDMS) replication techniques such as soft lithography [26], thermoplastic replication methods such as hot embossing and microinjection molding, microfluidic Tectonics [93] and micromachining techniques based on drilling, and Computer Numerical Control (CNC) machining using transparent thermoplastics (Poly-Methyl MethAcrylate, PMMA).

Photolithography

The method is based on the transfer of energy of light of certain wavelengths to specific photoactive materials on the substrate. The micro structure is transferred to the reactive liquid upon light exposure through a patterned photomask. The photoactive material undergoes a chemical reaction of liquid-solid transition due to the exposure to the light. After removing the unconverted reactive liquid and baking, a positive or negative structure of solid material will remain on the substrate. The benefits are mainly the possibility to control light spatially, and the ability to fabricate micro-sized structures directly through feature patterning or indirectly through fabrication of structured molds. The basic components of a photolithographic system are a UV light of 254-365 nm, a spin coater and a suitable substrate with related photoresist [94].

As shown in Figure 4.7, a solid substrate (glass or silicon) is spin-coated to apply a thin photoresist layer of 1-500 μm by the centrifugal force. After evaporation of the solvents in the photoresist via soft baking, the substrate is exposed to UV light through a high-resolution mask on plastic or glass film with the desired microfluidic pattern. After baking, depending on which photoresist is used, the un- or exposed layer of the photoresist is removed using chemical bath development, and the desired pattern remains on the substrate, thus forming a positive or negative mold. Traditionally, positive photoresists increase the solubility of the light-exposed areas while negative photoresists are insoluble in the exposed areas, which is more common in microfluidic applications as a negative mold for devices constructed from a different material.

The limitations of this technique are the poorer sealing quality, the invariable surface

chemistry and limitation to find photoresists that can be used with other substrates than silicon [95].

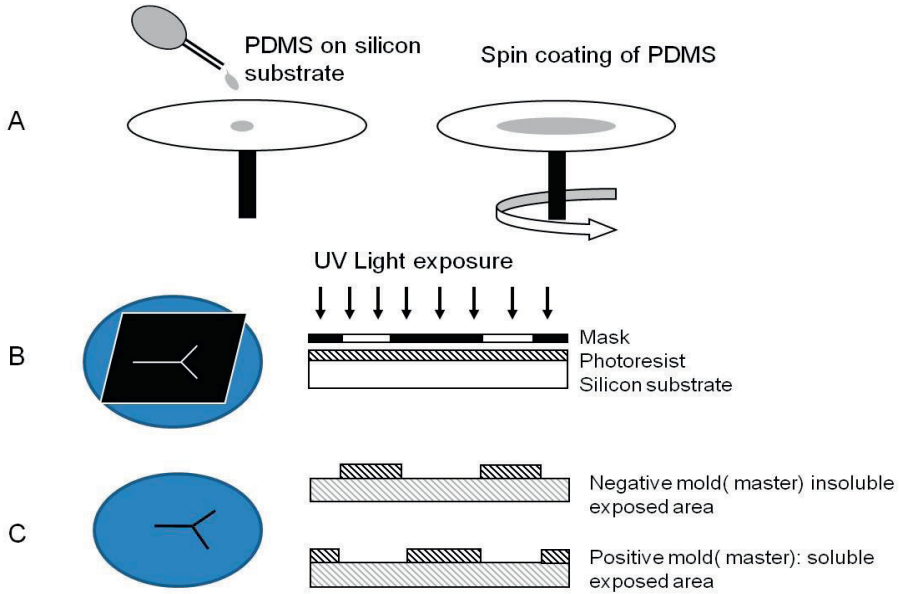


Figure 4.7: A) A photoresist is spin coated on a silicon substrate, B) The substrate with the spin-coated layer of photoresist is exposed to UV light through a high-resolution mask C) After baking and chemical developments, the non-crosslinked material is removed, resulting in either a negative or a positive mold.

Soft lithography

Soft lithography is a technique used to construct microstructures from Poly-DiMethyl Siloxane (PDMS) [96]. Typically, PDMS structures are formed from molding against a negative image of the desired structure. The mold can be fabricated in many different ways depending on the desired resolution and the number of replications that the mold must withstand. Thus, in applications with short prototyping series or variable designs, the molds are usually fabricated by photolithography. A typical production process is schematically described in Figure 4.7.

The resulting devices have many attractive properties, such as chemical inertness and facile bonding to glass or other layers of PDMS, i.e. multilayers which enable efficient fluid flow pumping schemes [97]. The surfaces can be modified compared to other materials to

achieve hydrophobic to hydrophilic transformations through oxygen plasma treatment. However, plasma-treated surfaces can maintain the hydrophilicity only for short-time laboratory experiments and device verification. The limitation of the quick hydrophobic recovery of PDMS surfaces has been addressed either by attaching larger molecules to the surface for increasable durability of the surface or by network forming modification to increase the surface stability [98].

The main disadvantages of soft lithography are the gas-permeability, the invariability, and that they are incompatible with non-polar solvents that may block the channels or cause cross contamination of adjacent fluidic streams. Furthermore, PDMS is usually thermally cured and patterned through material exclusion against a negative image mold. The connections, such as channels and reservoirs within the layer are often manually fabricated with needles placed before pouring the PDMS, as seen in Figure 4.8, or by hole-punching in the finished microfluidic device which may reduce the precision and repeatability.

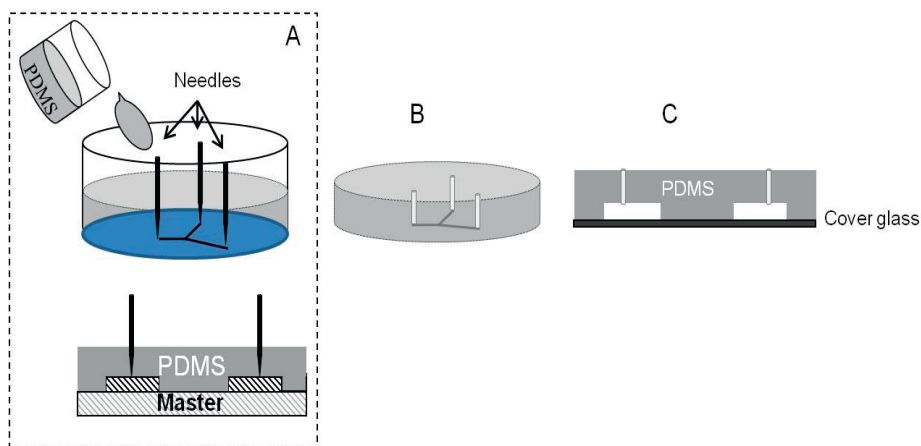


Figure 4.8: A) The needles are located in connection with the channels prior to the pouring of PDMS into the mold, B) The needles are removed and the finished microfluidic system is released from the mold after thermal curing, C) microfluidic system is placed on a cover glass.

Computer numerical control (CNC) micromachining

Conventional CNC micromachining techniques [99] are used for fabrication of PMMA-based microchips. The advantages are low cost of material, availability of CNC machines at universities or at commercial workshops, and the ease to create milled designs. The disadvantages are the poor surface quality, low yield strength, substrate hardness, and poor tolerances [100]. In addition, the inability to assemble the tolerances required for

analytical microchips with features $< 10\mu\text{m}$, is one of the most significant limiting factors in the use of CNC milling for lab-on-a-chip devices.

Most analytical microchips require features with dimensions on the order of 10-200 μm . Such tolerances are possible with CNC milling as a standard fabrication technique. The conventional CNC milling is used to fabricate prototype microchips for direct use or molds of harder materials for rapid generation of analytical microchip platforms via PDMS casting or hot embossing. Nowadays, the widely-used and novel key for using various milling techniques is the ability to combine bench-top microscopes to yield microchips with accurate tolerances on the order of 2-10 μm [99].

Prior to any milling, drilling, or cutting, the desired tolerances of the vertical and horizontal positions of the mill related to the surface of the block of PMMA or other materials should be adjusted. For accurate aspect ratio features, the depth of the feature, z-axis, is pre-calibrated to absolute zero to control. The size and shape of the desired micro channels are achieved by using cutter drills with different tips related to the desired features. To achieve the best tolerances, test modules are pre-fabricated and investigated under commercial microscopes to monitor the desired sizes and features.

4.3.4 Applications of Microfluidic systems

The main applications of microfluidic systems related to biological investigations are shown in DNA analysis including polymerase chain reaction (PCR) [101-108], sample preparation [109], highly sensitive enzyme analyses [110-115], high-throughput screening (HTS) (i.e., mixing, reaction, and separation) [116-121], cellular analysis such as micro-flow cytometry devices to sort, analyze, and count cells [122-127], cell-based microchips for high-throughput analysis [128-129], cell-based biosensors for multiple physiological responses of cells to environments [130-132], culturing systems including cell-cell, cell-substrate, and cell-medium interactions with a high degree of precision [133-134].

4.4 Optical spectroscopy

Optical spectroscopic techniques measure the spectral response of the interaction of light with substances as a function of wavelength or frequency. The techniques are classified related to the used light source and the nature of the interaction between the energy and the material [135].

4.4.1 Absorption Spectroscopy

In Ultraviolet-visible (UV-Vis) absorption spectroscopy, absorption occurs when the energy of the absorbed light matches the energy required for a specific molecule to undergo an electronic transition from the ground state to one or more higher excited states, as seen in Figure 4.9B [136].

The Beer-Lambert law is often used in absorbance spectroscopy to determine quantitatively the transmittance $T = I/I_o$ or the absorbance $A = -\lg(T)$ from the incident

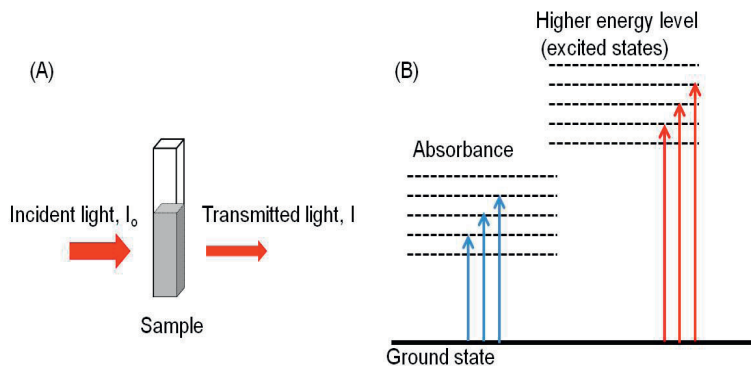


Figure 4.9: A) The incident light, I_o , and the transmitted light, I , through the sample, B) Electronic transitions for light absorbed by a molecule.

light I_o on the sample and the transmitted light I through the sample. The absorbance of a solution at the low states is directly proportional to the concentration of the absorbing species within the solution and the path length of light, and defined as:

$$A = \lg_{10} \frac{I_o}{I} = \epsilon c L \quad (4.6)$$

where A is the absorbance, I_o and I are the intensity of the incident and transmitted light, respectively, L is the path length of the light through the sample, c the concentration of the absorbing species in the solution, and ϵ is the constant molar absorptivity, which is defined for specific species and wavelengths in a given solvent, at a particular temperature and pressure, See Figure 4.9A. However, for a few complex molecules such as organic dyes (Xylenol Orange or Neutral Red) a 2nd order polynomial relationship between absorption and concentration is involved instead of the Beer-Lambert law [137].

4.4.2 The experimental setup

Conventionally, spectrophotometers are designed with a single beam, measuring the intensity I_o by removing, and then measuring the intensity I by placing the sample in the light beam or for dual beam configurations by splitting the light into two beams. Then both I and I_o are measured simultaneously.

Figure 4.10 shows the diagram of a typical dual beam spectrophotometer with a continuous light source, a diffraction grating in a monochromator or a prism to split the light into different wavelength, a holder for the sample, and a detector.

The light beam is first split into a bundle of monochromatic wavelengths by a prism or a diffraction grating. A half-mirrored device splits a single monochromatic beam into two

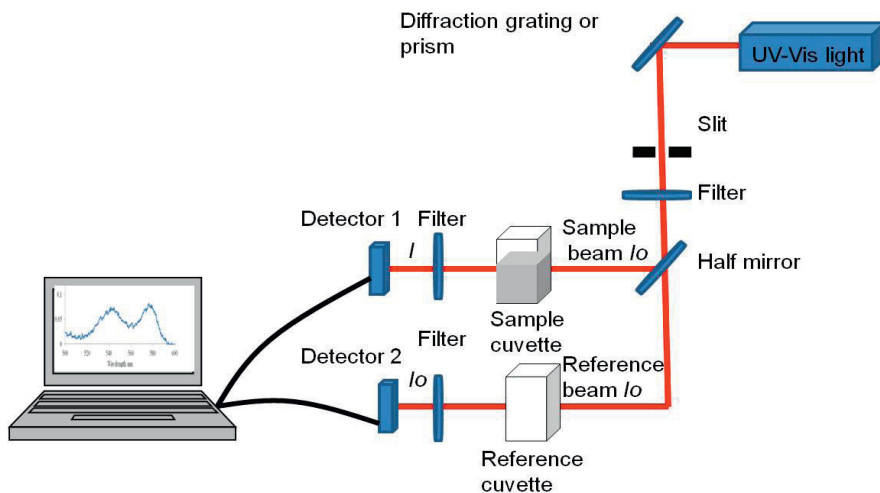


Figure 4.10: A schematic setup of typical dual beam spectrometer with the following components; UV-Vis light source, pin hole (slit), filters, diffraction grating or prism, sample holders(cuvette) and detectors connected to computer for spectra analysis and imaging.

beams with equal intensities. A sample beam passes through a transparent cuvette with a sample and another reference beam passes through an identical cuvette without sample. The intensity of the light beams are then measured and compared by the detector. The absorption is then, after analysis, shown as an absorption spectrum on the monitor.

4.4.3 Applications of UV-Vis spectroscopy

UV-Vis spectroscopy has mainly been used in analytical chemistry for the quantitative determination of different microscopic samples and analytes, such as transition metal ions, highly conjugated organic compounds [138], and biological macromolecules. The technique is widely used to analyze the dyes and pigments in individual textile fibers [139], microscopic paint chips [140] and the color of glass fragments, to determine the energy content of coal and petroleum source rock by measuring the vitrinite reflectance, and to monitor and quality control the thickness of the deposited thin films in the semiconductor and micro-optics industries [141]. Related to our work, hemoprotein analysis [142-144] and protein assays for molecular biology [145-147] are important.

Methods and materials

This chapter gives a brief review of the materials and methods included in the experimental setup. The integration of the patch-clamp micropipette for electrophysiological measurements in the microfluidic chamber, the optical manipulation of single biological cells in the microchannels, and the spectroscopic measurements under varying environments will be described.

5.1 Experimental setup

5.1.1 Preparations of biological cells and solutions

The experiments were initially performed using red blood cells (RBC) taken from a healthy volunteer, diluted in a solution of Phosphate-Buffered Saline (PBS). The deoxygenated solution was prepared by using Natriumdithionit, $Na_2O_4S_2$ (Sigma-Aldrich, USA), dissolved in 4 ml (PBS) solution. Latter experiments were performed on nerve cells prepared from the brains of Sprague Dawley rats prepared according to the ethical approval of the procedures given by the regional ethics committees for animal research ("Umeå djurförsöksetiska nämnd", approval No. A13-08 and A18-11).

The recording solutions were extracellular solutions (ECS) to flush the sample, prepared from chemical components to match the properties of fluids outside of the brain cells and intracellular solutions (ICS) that matched the fluid properties within the cell to fill the patch-clamp pipette. The deoxygenated (ECS) solution was prepared by bubbling the ECS with nitrogen gas for 1 hour prior to the experiment within a gas-tight glass-container.

5.1.2 Design of a microchip with integrated pipette combined with optical tweezers and UV-Vis spectroscopy

Papers A and B show the experimental setup built on an inverted optical microscope (IX 71, Olympus, Japan) placed on a vibration-isolated table (TechnicalManufacturing

Corporation, TMC, USA).

The optical tweezers apparatus was built upon an NIR-diode laser (Lasiris, StockerYale, USA), operating at 830 nm with a power of 150 mW. In our alternative design, the two positive lenses were mounted on two XYZ-translation stages (Thorlabs, USA), and both were used for the beam expansion and beam steering by adjusting the distance between them.

A UV-Vis spectrometer (Ocean Optics, HR4000, USA) was integrated to monitor the oxygenation states by recording absorption spectra of single optically trapped RBCs. The microscope light transmitted through the sample was collected by the microscope objective and the dichroic mirror, and then split by a beam-splitter to the CCD for imaging and the UV-Vis spectrometer for absorption spectra measurements through an optical fiber.

In paper A, the concept of PDMS-based microfluidic chip with an integrated patch-clamp micropipette was demonstrated. A pipette-like metal needle was located through tubing within the microfluidic channel before pouring PDMS. After finishing the microchip the needle was removed and the micropipette was inserted while avoiding sealing or damaging the tip of the pipette. To position the micropipette on a desired positive channel on the master before pouring PDMS, metal micropipette-like needles were inserted in contact with the desired positive microchannel on the silicon wafer. The designed cylinder-shaped holder ensured the stability of the pipette and operated as a mould for the fabrication of the PDMS. The holder designed with holes was placed over the external cylindrical area. The holes were pointed to different positions on the master corresponding to the different mould depths. This special holder enabled a precise positioning of the needle tip on a desired point, i.e. the channel where the biological cell was to be investigated, on the rotatable silicon master, see Figure 5.1. The resulting

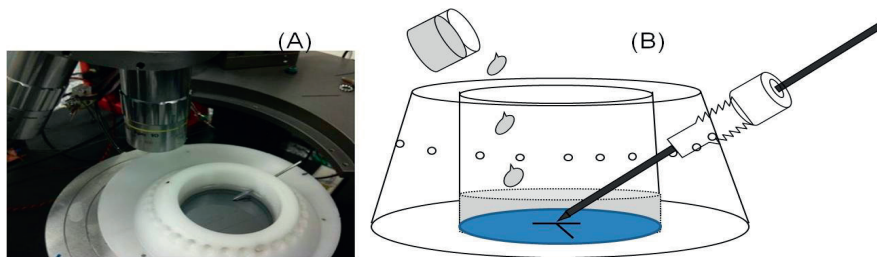


Figure 5.1: A) PDMS-based microfluidic chamber with a pipette-like needle for integration of a patch-clamp micropipette. B) Schematic figure of the pipette integration within a PDMS-based microchip.

microchip was placed under the inverted microscope equipped with optical tweezers. The injection of the biological cells and variations of the environment were generated by a pump-driven flow. A single RBC was selected, trapped and optically steered through the

microchannels towards the tip of the micropipette. Spectroscopic measurements were performed under variations of the oxygen content.

In paper B, the experimental setup presented earlier was modified by using an NIR-diode laser (IQ1A, Power Technology, USA), operating at 808 nm with an average power of 200 mW. A new model of the closed microfluidic chip of PMMA material was designed using micromatching fabrication by CNC (Circuit Board Milling) Machine. The microfluidic channels were structured on the PMMA block (100x70x20mm) and sealed by a cover glass using high quality adhesive epoxy. The CNC drilling technique was used to integrate the micropipette within the microchip to create micro-sized microfluidic channels and reservoirs, and in- and outlets were connected to the micro channels, see Figure 5.2.

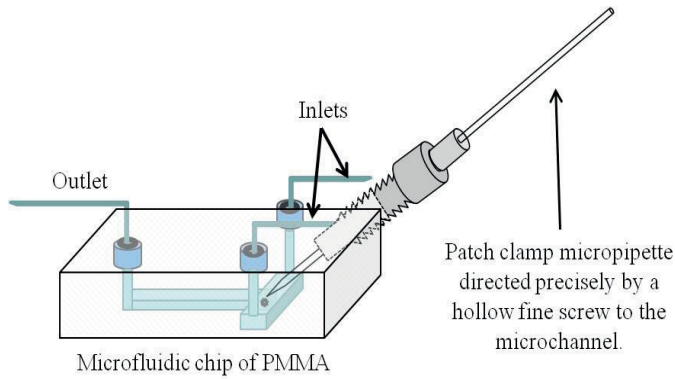


Figure 5.2: PMMA-based microfluidic chamber including integrated patch-clamp pipette.

The reasons for using this technique were mainly the high impermeability to air of PMMA and the ease of fabrication. The new microchip was designed with channel diameters of 900 μm for larger types of biological cells such as neurons. The new system allowed for simple and accurate positioning of the micropipette, exceptional monitoring of the sample, and airtight sealing. In addition, the system enabled integration of other techniques to the PMMA-based platform on the microscope such as optical spectroscopic techniques to measure the spectral response of the biological cell while interacted with light as a function of wavelength or frequency.

5.1.3 Electrophysiological investigations of single neurons

The concept of the multifunctional system presented in papers A and B was customized for patch-clamp electrophysiological investigations on single nerve cells. The experimental setup was built on an inverted microscope (Axiovert 25 CFL, Carl Zeiss, Germany) mounted on an optical table. An improved model of the microfluidic chip was fabricated

with a multi-channel system. The microchannels were constructed with approximately $100\ \mu\text{m}$ depth and $100\ \mu\text{m}$ width, connected to inlets and outlets adjacent to the channels to gastight tubing attached to two external pump systems for the infusion of both cells and different buffers. For integration of the patch-clamp technique, the microfluidic chip was fitted on a lab-designed stage on the microscope, as shown in Figure 5.3.

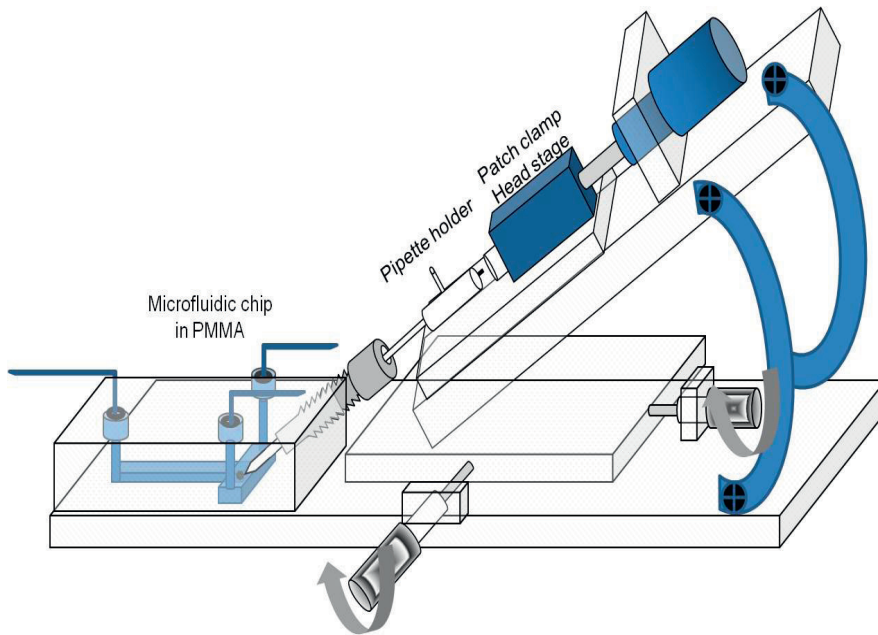


Figure 5.3: Microfluidic chip fitted on a lab-designed stage on the microscope and connected to a patch-clamp head stage.

The micropipette was initially fitted into the specified position inside the microchannel by the sealed hollow screw. Thereafter, the pipette was connected to the patch-clamp amplifier through a pipette holder and a head stage and moved towards the cell within the channel. The experimental setup is seen in Figure 5.4.

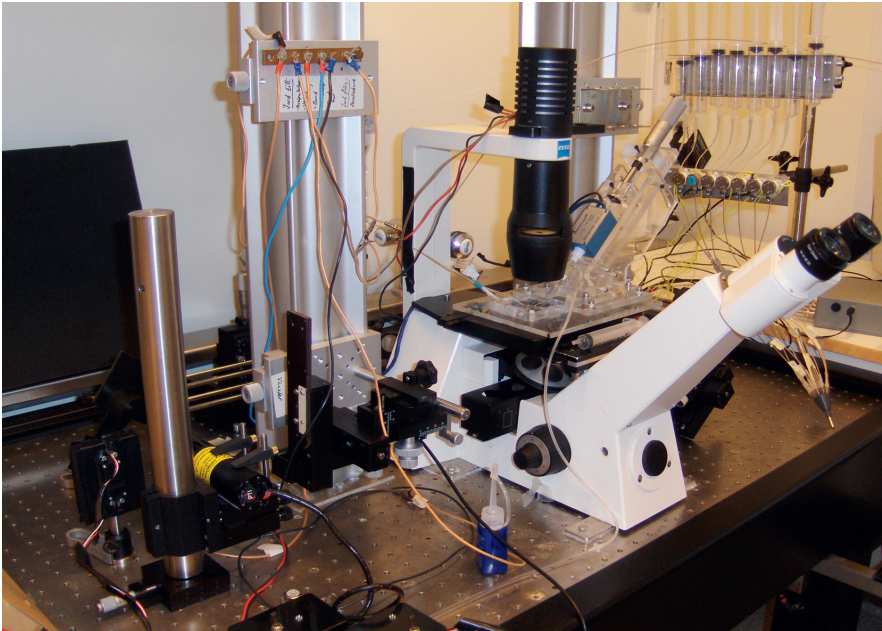


Figure 5.4: The experimental setup built on an inverted microscope, including patch-clamp, microfluidic chip and optical tweezers.

Results and discussions

6.1 Results and discussions

This chapter reviews the experimental results presented in papers A-C, including a comprehensive discussion of the significance of the multifunctional system to facilitate the electrophysiological investigations of single neurons under optimal control of the surrounding.

Paper A shows the first model of a closed microchip made out of PDMS with an integrated patch-clamp micropipette. The results showed that it was possible to introduce the cells and to change the environment of the cells by fluid flow rates obtained by a high precision pump system. Initially, the measurements were performed on optically manipulated single RBCs within the microfluidic channel that was brought in contact with the integrated patch-clamp pipette.

Experimentally, the fabrication procedures and the integration of the patch-clamp pipette were complicated and time consuming using soft lithography as presented in paper A. PDMS has a higher permeability to air compared to other materials such as glass, silicon or PMMA [148]. Despite the oxygen plasma treatment of PDMS surfaces, the hydrophilicity was maintained only for a short time, and the mass production of microchips for longer duration experiments was inaccessible due to the deformation or sealing of the channels. It should be mentioned that for patch-clamp investigations, the PDMS microchips could only be used one time since the micropipette has to be changed for each experiment. In addition, the process of creating macro-micro connections and reservoirs either previous to pouring the PDMS or afterwards, showed low precision and repeatability.

The drawbacks of the PDMS-based microchip were evaluated and a new model of a PMMA-based microchip was designed. The fabrication procedure was simplified as shown in paper B. The air-tightness of the microchip was evaluated during rapid changes of the environment by applying pressure-driven fluid flows.

The microchip was designed as a prototype for various electrophysiological investi-

gations of different types of cells with reliable control of the environment. The CNC designed microfluidic channel could be easily fabricated on PMMA or other suitable materials, which is beneficial due to the low cost, high efficiency, air-tight functionality, and high optical access. The results showed that the new functional design of the closed microchip with an integrated micropipette steered by the hollow screw enabled the monitoring of the micropipette entering the microfluidic channel. The microfluidic channels were connected through gas-tight tubing to the pump system. Single RBCs were optically manipulated through the microfluidic channel to the tip of the micropipette and monitored simultaneously. The micropipette was attached to the membrane of the trapped cell and monitored in real time. The spectroscopic measurements were done on the patched cell, and the absorption spectra were acquired under variations of different oxygenation states by the pump system as seen in Figure 6.1.

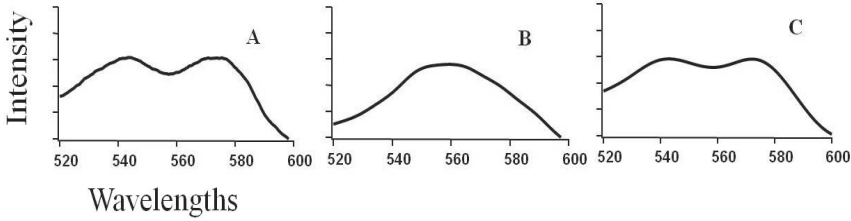


Figure 6.1: Absorption spectra of a single optically trapped RBC, in contact with the micropipette in the microfluidic system in (A) oxygenated state (B) deoxygenated state and (C) re-oxygenated state spectra are shown.

Further improvements were carried out on the first prototype for electrophysiological patch-clamp investigations of single neurons, as shown in paper C. The microfluidic channels were experimentally minimized to the 100- μm range and coated by UV curable epoxy for high glass-like optical transparency. The integration of the microchip included the micropipette fixed onto the patch-clamp head stage that was mounted onto the designed stage. This provided more degrees of freedom to position the pipette in 3-D within the microfluidic channel.

The system was evaluated by a series of experiments. Single RBCs were optically manipulated within the microfluidic channel system towards the integrated patch-clamp micropipette. Electrophysiological measurements of an optically trapped nerve cell in the open system were performed successfully, showing no remarkable influence of laser radiation on the patch-clamp measurements. The preliminary results showed sufficient control of rapid changes of cell environments within the microchip, and the oxygen level of the anoxic solution within the microchannels was measured to be as low as 1.0 ± 0.5 %. This was unachievable with the traditional "open-system" patch-clamp experiments where the oxygen content was 4.5 %.

The multifunctional system showed excellent potential to perform complete electrophysiological investigations on single neurons.

CHAPTER 7

Conclusions

This thesis reviewed the novel approach of combining a closed microfluidic system with an optical tweezers and optical spectroscopy to enable patch-clamp electrophysiological investigations.

The microfluidic chips were designed initially by soft lithography using PDMS material to enable the integration of a patch clamp pipette and to be used in a multifunctional system included optical tweezers and optical spectroscopy. Experiments were performed to transport the RBCs into the microfluidic chip, to trap and steer single RBCs optically through the microchannels towards the tip of the integrated pipette and to perform spectroscopic investigations while varying the oxygen saturation.

The method offered valuable experimental knowledge about the fluid flow behavior within the microfluidic system and mainly showed the proof of principle to be improved and used in the next experiments. The time-consuming and complex procedure to integrate the micropipette into the (single-use) PDMS-based microfluidic chip, was alleviated by designing a CNC machined (multi-used) PMMA-based microfluidic chip with an integrated micropipette. This microfluidic chip showed reduced air permeability and fabrication costs. The chip was experimentally verified to manipulate RBCs and nerve cells towards the micropipette while spectroscopic and electrophysiological measurements were performed under controllable oxygen conditions.

This designed closed lab-on-a-chip may act as a multifunctional system for simultaneous and high-throughput experiments, and it enables analysis of biological cells under environmental control during the measurements. The first measurements with the prototype showed promising results to select and trap single cells towards the micropipette where electrophysiological studies of single cells in an environment-controlled system can be performed.

CHAPTER 8

Future outlook

To enhance the performance of the microfluidic system, further improvements should be addressed to achieve better control of the cell transport to the microfluidic chamber. This can be realized by a modified design in which the cells are directly dissociated into the microfluidic chamber while cell transport through the microchannel would be achieved by applying a negative pressure. It is vital to minimize the stress that the cells experience during transport through long tubing.

The mobility and viability of neurons demand further investigations related to the fluid flow to enable improved cell sorting. The sticky tendency of the nerve cells onto the cover glass and the inner walls of the channels makes the cells inflexible and difficult to be trapped by the optical tweezers. Thus, the limitation should be investigated further either by newly designed channels or by coating the channels with anti-stick polymeric materials.

The ongoing approach is to enhance the viability of the nerve cells by optimizing the fluid flow profile, using a shorter path for cell-transport or by modifying the existing microfluidic chip to act as a Petri dish for direct dissociation of the cells from the brain tissue into the chamber. Furthermore, in another considered design, the pipette will be inserted to the microfluidic chip through a conical seal of gas-tight material attached by a suitable adhesive epoxy. This will enable the pipette to point at and attach to cells lying within the entire volume of the cellular solution. This microfluidic chip can be adapted in most patch-clamp configurations without expensive modifications.

Other considered improvements are to integrate Raman spectroscopy within the experimental setup to gain multiple information of the investigated nerve cell during the electrophysiological measurements.

The long-term goal is to study the response of individual neurons and defense mechanisms in hypoxic conditions that may establish new ways to understand cell behavior related to neuroglobin for various diseases such as stroke, Alzheimer's and Parkinson's.

CHAPTER 9

References

- [1] WHO, World Health Organization, global health risks, Mortality and burden of disease attributable to selected major risks Library Cataloguing-in-Publication Data, ISBN 978 92 4 156387 1, (2009).
- [2] A. M. Moskowitz, E. H. Lo and C. Iadecola, "The Science of Stroke: Mechanisms in Search of Treatments," *Neuron* 67(2), 181-198 (2010).
- [3] G. Del Zoppo and J. Marler, "Ischemic Stroke, Pathways to Treatment", ISBN: 9781405103671, (2009).
- [4] P. Lipton, "Ischemic Cell Death in Brain Neurons," *Physiol Rev* 79(4), 1431-156 (1999).
- [5] N. B. Slonim, and L. H. Hamilton, "Blood-Gas Transport" *Respiratory, Physiology* 5th Ed., C.V. Mosby Co., 135-153 (1987).
- [6] A. C. Guyton, and J. E. Hall, "Transport of Oxygen and Carbon Dioxide in the Blood and Body Fluids," *Medical Physiology*, 10th Ed., WB Saunders Company, 463-473 (2000).
- [7] T. Burmester, B. Weich, S. Reinhardt and T. Hankeln, "A vertebrate globin expressed in the brain," *Nature* 407, 520-523 (2000).
- [8] A. A. Khan, A. A. Wang, Y. Sun et al., "Neuroglobin-overexpressing transgenic mice are resistant to cerebral and myocardial ischemia," *PNAS* 103(47), 17944-17948 (2006)
- [9] T. Hankeln, B. Ebner, C. Fuchs et. al, "Neuroglobin and cytoglobin in search of their role in vertebrate globin family," *J. Inorg. Biochem.* 99, 110-119 (2005).
- [10] J. M. Kriegl, A. J. Bhattacharyya, K. Nienhaus et al., "Ligand binding and protein dynamics in neuroglobin," *Proc. Natl. Acad. Sci., USA*, 99, 7992-7997 (2002).
- [11] M. Schmidt, A. Giessel, T. Laufs, T. Hankeln et al., "How Does the Eye Breathe? Evidence for neuroglobin-mediated oxygen supply in the mammalian retina," *J. Biol. Chem.* 278, 1932-1935 (2003).
- [12] E. Geuens, I. Brouns, D. Flamez, S. Dewilde et al., "A globin in the nucleus," *J. Biol. Chem.* 278, 30417-30420 (2003).

- [13] S. Wystub, T. Laufs, M. Schmidt, T. Burmester et al., "Localization of neuroglobin protein in the mouse brain," *Neurosci. Letts.* 346, 114-116 (2003).
- [14] M. Brunori and B. Vallone, "Neuroglobin, seven years after," *Cell Mol Life Sci.* 64, 1259-1268 (2007).
- [15] Y. Sun, K. Jin, X. O. Mao, Y. Zhu and D. A. Greenberg, "Neuroglobin is up-regulated by and protects neurons from hypoxic-ischemic injury," *PNAS* 98(26), 15306-15311 (2001).
- [16] R. C. Li, S. K. Lee, F. Pouranfar, K. R. Brittian et al., "Hypoxia differentially regulates the expression of neuroglobin and cytoglobin in rat brain," *Brainresearch* 1096, 173-179 (2006).
- [17] Y. Zhao, S. Inayat, D. A. Dikin, J. H. Singer, R. S. Ruoff, and J. B. Troy, "Patch clamp technique: review of the current state of the art and potential contributions from nanoengineering," *Proc. IMechE J. Nanoengineering and Nanosystems* 222, 1-11 (2008).
- [18] A. Brüggemann, C. Farre, C. Haarmann, A. Haythornthwaite, M. Kreir et al., "Planar patch clamp: advances in electrophysiology". *Methods Mol Biol.* 491, 165-176 (2008).
- [19] J. C. Behrends, N. Fertig, "Neuromethods: patch-clamp analysis advanced techniques," 2nd Ed., Wolfgang Walz, Humana Press: Totowa, N.J. 38, 411-433 (2007).
- [20] H. Andersson and A. van den Berg, "Microfluidic devices for cellomics: a review," *Sens. Actuators B Chem.* 92, 315-325 (2003).
- [21] D. N. Breslauer, P. J. Lee and L. P. Lee, "Microfluidics-based systems biology," *Mol. Biosys.* 2, 97-112 (2006).
- [22] S. Britland, P. Clark, P. Connolly and G. Moores, "Micropatterned substratum adhesiveness a model for morphogenetic cues controlling cell behavior," *Exp. Cell Res.* 198, 124-129 (1992).
- [23] C. S. Chen, M. Mrksich, S. Huang, G. M. Whitesides and D. E. Ingber, "Geometric control of cell life and death," *Science* 276, 1425-1428 (1997).
- [24] N. Gomathi, A. Sureshkumar and S. Neogi, "RF plasma-treated polymers for biomedical applications," *Current science* 94(11), 1478-1486 (2008).
- [25] L. Yao, B. Liu, T. Chen, S. Liu and T. Zuo, "Micro flow-through PCR in a PMMA chip fabricated by KrF excimer laser," *Biomed. Microdevices* 7(3), 253-257 (2005).
- [26] Y. Xia and G. M. Whitesides, "Soft lithography," *Annu. Rev. Mater. Sci.* 28(1), 153-184 (1998).
- [27] H. Y. Tan, W. K. Loke and N.T. Nguyen, "A reliable method for bonding polydimethylsiloxane (PDMS) to polymethylmethacrylate (PMMA) and its application in micropumps," *Sensors and Actuators B: Chemical* 151(1), 133-139 (2010).
- [28] S. Balslev, A. M. Jorgensen, B. Bilenberg, K. B. Mogensen et al., "Lab-on-a-chip with integrated optical transducers," *Lab Chip* 6(2), 213-217 (2006).
- [29] H. Qi, X. Wang, T. Chen, X. Ma and T. Zuo, "Fabrication and characterization of a polymethyl methacrylate continuous-flow PCR microfluidic chip using CO_2 laser ablation," *Microsyst. Technol.* 15(7), 1027-1030 (2009).
- [30] P. Liuni, T. Rob, and D. J. Wilson, "A microfluidic reactor for rapid, low-pressure proteolysis with on-chip electrospray ionization," *Rapid Commun. Mass Spectrom.*

24(3), 315-320 (2010).

- [31] G. B. Lee, S. H. Chen, G. R. Huang, W. C. Sung and Y. H. Lin, "Microfabricated plastic chips by hot embossing methods and their applications for DNA separation and detection," *Sens. Actuators B Chem.* 75(1-2), 142-148 (2001).
- [32] A. Ashkin, J. M. Dziedzic and T. Yamane, "Optical trapping and manipulation of single cells using infrared laser beams," *Nature* 330(6150), 769-771 (1987).
- [33] T. M. Squires and S. R. Quake, "Microfluidics: Fluid physics at the nanoliter scale," *Rev. Mod. Phys.* 77(3), 977-1026 (2005).
- [34] E. Eriksson, J. Scrimgeour, A. Graneli, K. Ramser et al., "Optical manipulation and microfluidics for studies of single cell dynamics," *J. Opt. A: Pure Appl. Opt.* 9, 113-121 (2007).
- [35] S. Chu, J. E. Bjorkholm, A. Ashkin and A. Cable, "Experimental observation of optically trapped atoms," *Phys. Rev. Lett.* 57(3), 314-317 (1986).
- [36] A. Ashkin, K. Schütze, J. M. Dziedzic, U. Euteneuer and M. Schliwa, "Force generation of organelle transport measured in vivo by an infrared laser trap," *Nature* 348(6299), 346-348 (1990).
- [37] J. Yang, Y. Huang, X. B. Wang, F. F. Becker, and P. R. C. Gascoyne, "Cell separation on microfabricated electrodes using dielectrophoretic/gravitational field-flow fractionation," *Anal. Chem.* 71(5), 911-918 (1999).
- [38] I. K. Glasgow, H. C. Zeringue, D. J. Beebe, S. J. Choi, J. T. Lyman et al., "Handling individual mammalian embryos using microfluidics," *IEEE Trans. Biomed. Eng.* 48(5), 570-578 (2001).
- [39] D. Figeys, S. P. Gygi, G. McKinnon and R. Aebersold, "An integrated microfluidics-tandem mass spectrometry system for automated protein analysis," *Anal. Chem.* 70(18), 3728-3734 (1998).
- [40] Z. H. Fan, S. Mangru, R. Granzow, P. Heaney et al., "Dynamic DNA hybridization on a chip using paramagnetic beads," *Anal. Chem.* 71(21), 4851-4859 (1999).
- [41] D. D. Cunningham, "Fluidics and sample handling in clinical chemical analysis," *Anal. Chim. Acta* 429(1), 1-18 (2001).
- [42] W. W. Hellmich, C. Pelargus, K. Leffhalm, A. Ros and D. Anselmetti, "Single cell manipulation, analytics, and label-free protein detection in microfluidic devices for systems nanobiology," *Electrophoresis* 26(19), 3689-3696 (2005).
- [43] J. P. Shelby, S. A. Mutch and D. T. Chiu, "Direct manipulation and observation of the rotational motion of single optically trapped microparticles and biological cells in microvortices," *Anal. Chem.* 76, 2492-2497 (2004).
- [44] K. Ramser and D. Hanstorp, "Optical manipulation for single-cell studies," *J. Biophotonics* 3(4), 187-206 (2010).
- [45] K. Schütze, H. Pösl and G. Lahr, "Laser micromanipulation systems as universal tools in cellular and molecular biology and in medicine," *Cell. Mol. Biol.* 44(5), 735-746 (1998).
- [46] N. R. Munce, J. Li, P. R. Herman and L. Lilge, "Microfabricated system for parallel single-cell capillary electrophoresis," *Anal. Chem.* 76(17), 4983-4989 (2004).
- [47] R. Malhotra et al., "Hypoxia induces apoptosis via two independent pathways in

- Jurkat cells: differential regulation by glucose," *Am J Physiol Cell Physiol.* 281(5), C1596-1603 (2001).
- [48] W. R. Mattiesen et al., "Increased neurogenesis after hypoxic-ischemic encephalopathy in humans is age related," *Acta Neuropathol.* 117(5), 525-534 (2009).
- [49] J. Lapointe and G. Szabo, "A novel holder allowing internal perfusion of patch-clamp pipettes," *Pflügers Arch, J. of Physiology* 405(3), 285-293 (1985).
- [50] B. Sakmann and E. Neher, "Patch Clamp Techniques for Studying Ionic Channels in Excitable Membranes," *Ann. Rev. of Phys.* 46, 455-472 (1984).
- [51] P. Avi, G. Ziv, T. Vincent, Y. Moy et al., "Ionic Requirements for Membrane-Glass Adhesion and Giga Seal Formation in Patch-Clamp Recording," *Biophys.* 92(11), 3893-3900 (2007).
- [52] L. Kiss, P. Bennett, V. N. Uebele, et al., "High throughput ion-channel pharmacology: planar-array-based voltage clamp," *Assay Drug Dev. Technol.* 1, 127-135, (2003).
- [53] M. J. Lang and S. M. Block, "Laser-based optical tweezers," *Am. J. Phys.* 71, 201-215 (2003).
- [54] A. Ashkin, "Optical trapping and manipulation of neutral particles using lasers," *Proc. Natl. Acad. Sci.* 94, 4853-4860 (1997).
- [55] M. P. Sheetz, L. Wilson and P. Matsudaira, "Laser Tweezers in Cell Biology," *Methods in Cell Biology* Ed. Vol (55), New York, Academic Press. 223 (1998).
- [56] K. C. Neuman and S. M. Block, "Optical trapping," *Rev. Scientific Instruments* 75(9), 2787-2809 (2004).
- [57] A. Ashkin, "Forces of a single-beam gradient laser trap on a dielectric sphere in the ray optics regime," *J. Biophys.* 61(2), 569-582 (1992).
- [58] A. Ashkin, J. M. Dziedzic, J. E. Bjorkholm and S. Chu, "Observation of a single-beam gradient force optical trap for dielectric particles," *Optics lett.* 11(5), 288-290 (1986).
- [59] A. Cox and J. Linden, "An experiment to measure mie and rayleigh total scattering cross sections," *Am. J. physics* 70, 620-625 (2002).
- [60] A. Rohrbacha and E. H. Stelzerb, "Three-dimensional position detection of optically trapped dielectric particles," *J. of appl. Phys.* 91(8), 5474-5488 (2002).
- [61] M. Steven and M. Block, "Making light work with optical tweezers," *Nature* 360, 493-495 (1992).
- [62] C. D'Helon, E. W. Dearden, H. Rubinsztein-Dunlop and N. R. Heckenberg, "Measurement of the optical force and trapping range of a single-beam gradient optical trap for micronsized latex spheres," *J. Mod. Optics* 41(3), 595-601 (1994).
- [63] K. C. Neuman et al., "Characterization of photodamage to *Escherichia coli* in optical traps," *Biophysical Journal* 77(5), 2856-2863 (1999).
- [64] S. Chu, "Laser manipulation of atoms and particles," *Science* 253, 861-866 (1991).
- [65] J. W. Shaevitz, "A Practical Guide to Optical Trapping," 1-19 (2006).
- [66] M. P. MacDonald, G. C. Spalding and K. Dholakia, "Microfluidic sorting in an optical lattice," *Nature* 426(6965), 421-424 (2003).
- [67] N. Thomas and R. A. Thornhill, "The physics of biological molecular motors," *J. physics D-applied physics* 31(3), 253-266 (1998).

-
- [68] E. M. Bonder et al., "Force production by swimming sperm analysis using optical tweezers," *Journal of Cell Biology* 111(5-2), 421-472 (1990).
 - [69] H. Clausen-Schaumann et al., "Mechanical stability of single DNA molecules," *Biophysical Journal* 78(4), 1997-2007 (2000).
 - [70] R. Rohs, C. Etchebest and R. Lavery, "Unraveling proteins: A molecular mechanics study," *Biophysical Journal* 76(5), 2760-2768 (1999).
 - [71] A. E. M. Clemen et al., "Force-dependent stepping kinetics of myosin-V," *Biophysical Journal* 88(6), 4402-4410 (2005).
 - [72] S. M. Block, "Nanometers and piconewtons - the macromolecular mechanics of kinesin," *Trends in cell biology* 5(4), 169-175 (1995).
 - [73] M. Arya et al., "Measurement of the binding forces between vonWillebrand factor and variants of platelet glycoprotein Ib alpha using optical tweezers," *Lasers in Surgery and Medicine* 30(4), 306-312 (2002).
 - [74] S. Seeger et al., "Application of laser optical tweezers in immunology and molecular genetics," *Cytometry* 12(6), 497-504 (1991).
 - [75] M. Ericsson et al., "Sorting out bacterial viability with optical tweezers," *Journal of bacteriology* 182(19), 5551-5555 (2000).
 - [76] J. Conia, B. S. Edwards and S. Voelkel, "The micro-robotic laboratory: Optical trapping and scissoring for the biologist," *Journal of clinical laboratory analysis* 11(1), 28-38 (1997).
 - [77] B. H. Weigl, R. L. Bardell and C. R. Cabrera, "Lab-on-a-chip for drug development," *Advanced Drug Delivery Reviews* 55(3), 349-377 (2003).
 - [78] I. G. Currie, "Fundamental mechanics of fluids," Marcel Dekker, Inc. (2003).
 - [79] C. Kim, K. Lee, J. H. Kim, K. S. Shin, K.-J. Lee, T. S. Kim and J. Y. Kang, "A serial dilution microfluidic device using a ladder network generating logarithmic or linear concentrations," *Lab Chip* 8, 473-479 (2008).
 - [80] www.cvphysiology.com/Hemodynamics/H006.htm.
 - [81] K. Avila, D. Moxey, A. De Lozar, M. Avila, D. Barkley and B. Hof, "The Onset of Turbulence in Pipe Flow," *Science* 333(6039), 192-196 (2011).
 - [82] T. E. Faber, "Fluid Dynamics for Physicists," Cambridge University Press, New York (1995).
 - [83] L. L. Sohn et al., "Capacitance cytometry: Measuring biological cells one by one," *Proc. National Academy Sciences U.S.A.* 97, 10687-10690 (2000).
 - [84] M. L. Kovarik, H. H. Lai, J. C. Xiong and N. L. Allbritton, "Sample transport and electrokinetic injection in a microchip device for chemical cytometry," *Electrophoresis* 32, 1-8 (2011).
 - [85] R. Yang et al., "Microfabrication and test of a three-dimensional polymer hydro-focusing unit for flow cytometry applications," *Sensors Actuators A* 118, 259-267 (2005).
 - [86] B. H. Weigl and P. Yager, "Microfluidic diffusion-based separation and detection," *Science* 283, 346-347 (1999).
 - [87] M. A. Burns, B. N. Johnson, S. N. Brahmasandra, K. Handique, J. R. Webster et al., "An Integrated Nanoliter DNA Analysis Device," *Science* 282(5388), 484-487 (1998).
 - [88] G. Ocvirk, M. Munroe, T. Tang, R. Oleschuk, K. Westra and D. J. Harrison, "Elec-

- trokinetic control of fluid flow in native poly(dimethylsiloxane) capillary electrophoresis devices," *Electrophoresis* 21(1), 107-115 (2000).
- [89] J. Clemmens et al., "Motor-protein "roundabouts": microtubules moving on kinesin-coated tracks through engineered networks," *Lab Chip* 4(2), 83-86 (2004).
- [90] U. Tallarek, E. Rapp, T. Scheenen, E. Bayer and H. Van As, "Electroosmotic and pressure-driven flow in open and packed capillaries," *Anal. Chem.* 72, 2292-2301 (2000).
- [91] P. A. Thompson and S. M. Troian, "A general boundary condition for liquid flow at solid Surfaces," *Nature* 389, 360-362 (1997).
- [92] Celectricon, Gothenburg, Sweden, (<http://www.cellectricon.se>) and Fluidigm, CA, USA (<http://www.fluidigm.com>).
- [93] D. J. Beebe, J. S. Moore, Q. Yu, R. H. Liu, M. L. Kraft, B. H. Jo and C. Devadoss, "Microfluidic tectonics: A comprehensive platform for microfluidic systems," *Proceedings of the National Academy of Sciences U.S.A.* 97, 13488-13493 (2000).
- [94] C. H. Yu, A. N. Parikh and J. T. Groves, "Direct patterning of membrane-derivatized colloids using insitu UV-ozone photolithography," *Advanced Materials* 17, 1477-1480 (2005).
- [95] M. S. Yang, C. W. Li and J. Yang, "Cell docking and on-chip monitoring of cellular reactions with a controlled concentration gradient on a microfluidic device," *Analytical Chemistry* 74, 3991-4001 (2002).
- [96] S. J. Clarson and J. A. Semlyen "Siloxane Polymers," Englewood Cliffs, NJ: Prentice Hall (1993).
- [97] P. Kim, H. E. Jeong, A. Khademhosseini and K. Y. Suh, "Fabrication of non-biofouling polyethylene glycol micro- and nanochannels by ultraviolet-assisted irreversible sealing," *Lab Chip* 6, 1432-1437 (2006).
- [98] W. B. Hu, "Surface grafting on polymer surface using physisorbed free radical initiators," *Macromolecules*, 38(15), 6592-6597 (2005).
- [99] J. S. Mecomber, A. M. Stalcup, D. Hurd, H. Brian et al., "Analytical Performance of Polymer-Based Microfluidic Devices Fabricated By Computer Numerical Controlled Machining" *Anal. Chem.* 78, 936-941 (2006).
- [100] J. S. Mecomber, D. Hurd and P. A. Limbach, "Analytical Performance of Polymer-Based Microfluidic Devices Fabricated By Computer Numerical Controlled Machining," *Int. J. Machine Tools Manu.* 45, 1542-1550 (2005).
- [101] M. Shoffner, J. Cheng, G. Hvichia, L. Kricka and P. Wilding, "Chip PCR. I. Surface passivation of microfabricated siliconglass chips for PCR," *Nucleic Acids Res.* 24, 375-379 (1996).
- [102] J. Cheng, M. Shoffner, G. Hvichia, L. Kricka and P. Wilding, "Chip PCR. II. Investigation of different PCR amplification systems in microfabricated silicon-glass chips," *Nucleic Acids Res.* 24, 380-385 (1996).
- [103] T. Taylor, E. Winn-Deen, E. Picozza, T. Woudenberg and M. Albin, "Optimization of the performance of the polymerase chain reaction in silicon-based micro-structures," *Nucleic Acids Res.* 25, 3164-3168 (1997).
- [104] M. Kopp, A. De Mello and A. Manz, "Chemical amplification: continuous-flow PCR on a chip," *Science* 280, 1046-1048 (1998).

-
- [105] B. Giordano, J. Ferrance, S. Swedberg, A. Huhmer and J. Landers, "Polymerase chain reaction in polymeric microchips: DNA amplification in less than 240 seconds," *Anal. Biochem.* 291, 124-132 (2001).
- [106] P. Wilding, L. Kricka, J. Cheng, G. Hvichia, M. Shoffner and P. Fortina, "Integrated cell isolation and polymerase chain reaction analysis using silicon microfilter chambers," *Anal. Biochem.* 257, 95-100 (1998).
- [107] J. Hong, T. Fujii, M. Seki, T. Yamamoto and I. Endo, "PDMS [polydimethylsiloxane]-glass hybrid microchip for gene amplification," *Microtechnologies in Medicine and Biology*, Annual Int. Conference 170, 407-410 (2000).
- [108] S. Jacobson and J. Ramsey, "Integrated microdevice for DNA restriction fragment analysis," *Anal. Chem.* 68, 720-723 (1996).
- [109] P. Yuen, L. Kricka, P. Fortina, N. Panaro, T. Sakazume and P. Wilding, "Microchip module for blood sample preparation and nucleic acid amplification reactions," *Genome Res.* 11, 405-412 (2001).
- [110] I. Moser, G. Jobst, P. Svasek, M. Varahram and G. Urban, "Rapid liver enzyme assay with miniaturized liquid handling system comprising thin film biosensor array," *Sens. Actuators B* 44, 377-380 (1997).
- [111] A. Hadd, D. Raymond, J. Halliwell, S. Jacobson and J. Ramsey, "Microchip device for performing enzyme assays," *Anal. Chem.* 69, 3407-3412 (1997).
- [112] C. B. Cohen, E. Chin-Dixon, S. Jeong and T. Nikiforov, "A microchip-based enzyme assay for protein kinase A," *Anal. Biochem.* 273, 89-97 (1999).
- [113] A. Hadd, S. Jacobson and J. Ramsey, "Microfluidic assays of acetylcholinesterase inhibitors," *Anal. Chem.* 71, 5206-5212 (1999).
- [114] D. Duffy, H. Gillis, J. Lin, N. Sheppard and G. Kellogg, "Microfabricated centrifugal microfluidic systems: characterization and multiple enzymatic assays," *Anal. Chem.* 71, 4669-4678 (1999).
- [115] E. Schilling, A. Kamholz and P. Yager, "Cell lysis and protein extraction in a microfluidic device with detection by a fluorogenic enzyme assay," *Anal. Chem.* 74(8), 1798-1804 (2002).
- [116] L. Koutny, D. Schmalzing, T. Taylor and M. Fuchs, "Microchip electrophoretic immunoassay for serum cortisol," *Anal. Chem.* 68, 18-22 (1996).
- [117] F. Heeren, E. Verpoorte, A. Manz and W. Thormann, "Micellar electrokinetic chromatography separations and analyses of biological samples on a cyclic planar microstructure," *Anal. Chem.* 68, 2044-2053 (1996).
- [118] N. Chiem and D. Harrison, "Microchipbased capillary electrophoresis for immunoassays: analysis of monoclonal antibodies and theophylline," *Anal. Chem.* 69, 373-378 (1997).
- [119] D. Schmalzing, L. Koutny, T. Taylor, W. Nashabeh and M. Fuchs, "Immunoassay for thyroxine [T4] in serum using capillary electrophoresis and micromachined devices," *J. Chromatogr. B* 697, 175-80 (1997).
- [120] S. Cheng, C. Skinner, J. Taylor, S. Attiya, W. Lee et al., "Development of a multichannel microfluidic analysis system employing affinity capillary electrophoresis for immunoassay," *Anal. Chem.* 73, 1472-1479 (2001).

- [121] N. Chiem and D. Harrison, "Microchip systems for immunoassay: an integrated immunoreactor with electrophoretic separation for serum theophylline determination," *Clin. Chem.* 44, 591-598 (1998).
- [122] R. Carlson, C. Gabel, S. Chan, R. Austin, J. Brody and J. Winkelman, "Self-sorting of white blood cells in a lattice," *Phys. Rev. Lett.* 79(11), 2149-2152 (1997).
- [123] S. Fiedler, S. Shirley, T. Schnelle and G. Fuhr, "Dielectrophoretic sorting of particles and cells in a microsystem," *Anal. Chem.* 70, 1909-1915 (1998).
- [124] P. Li and D. Harrison, "Transport, manipulation, and reaction of biological cells on-chip using electrokinetic effects," *Anal. Chem.* 69, 1564-1568 (1997).
- [125] D. Sobek, S. Senturia and M. Gray, "Microfabricated fused silica flow chambers for flow cytometry," In *Tech. Dig. Solid-State Sensor Actuator Worksh.*, Hilton Head Island, SC, 260-263 (1994).
- [126] A. Fu, C. Spence, A. Scherer, F. Arnold and S. Quake, "A microfabricated fluorescence-activated cell sorter," *Nat. Biotechnol.* 17, 1109-1111 (1999).
- [127] D. Schrum, C. Culbertson, S. Jacobson and J. Ramsey, "Microchip flow cytometry using electrokinetic focusing," *Anal. Chem.* 71, 4173-4177 (1999).
- [128] D. Beebe, "Microfabricated fluidic devices for single cell handling and analysis. In *Emerging Tools for Single Cell Analysis: Advances in Optical Measurement Technologies*," Ed. G. Durack, J. Robinson, New York: Wiley (2000).
- [129] S. Sundberg, "High-throughput and ultra-high-throughput screening: solution- and cell-based approaches," *Curr. Opin. Biotechnol.* 11, 47-53 (2000).
- [130] J. Pancrazio, J. Whelan, D. Borkholder, W. Ma and D. Stenger, "Development and application of cell-based biosensors," *Ann. Biomed. Eng.* 27, 697-711 (1999).
- [131] L. Bousse, "Whole cell biosensors," *Sens. Actuators B* 34, 270-275 (1996).
- [132] T. Vo-Dinh, B. Cullum and D. Stokes, "Nanosensors and biochips: frontiers in biomolecular diagnostics," *Sens. Actuators B* 74, 2-11 (2001).
- [133] A. Folch and M. Toner, "Microengineering of cellular interactions," *Annu. Rev. Biomed. Eng.* 2, 227-256 (2000).
- [134] I. Inoue, Y. Wakamoto, H. Moriguchi, K. Okano and K. Yasuda, "On-chip culture system for observation of isolated individual cells," *Lab Chip* 1, 50-55 (2001).
- [135] R. Richards-Kortum and E. Sevick-Muraca, "Quantitative optical spectroscopy for tissue diagnosis," *Annual Review of Physical Chemistry* 47, 555-606 (1996).
- [136] S. L. Upstone, "Ultraviolet/Visible Light Absorption Spectrophotometry in Clinical Chemistry," *Encyclopedia of Analytical Chemistry* R.A. Meyers Ed. 1699-1714 (2000).
- [137] D. A. Skoog, D. M. West and F. J. Holler, "Fundamentals of Analytical Chemistry," Saunders College Publishing, Fort Worth, US (1992).
- [138] D. A. Skoog et al., "Principles of Instrumental Analysis," 6th ed. Thomson Brooks/Cole., 349-351 (2007).
- [139] "Forensic Fiber Examination Guidelines," Scientific Working Group-Materials, <http://www.swgmat.org/Forensic%20Fiber%20Examination%20Guidelines.pdf>, (1999).
- [140] M. Bacci, A. Orlando, M. Picollo, B. Radicati et al., "Colour analysis of historical red lakes using non-destructive reflectance spectroscopy. Compatible Materials for the Protection of Cultural Heritage," *PACT* 58, 21-35 (2000).

-
- [141] M. Horie, N. Fujiwara, M. Kokubo and N. Kondo, "Spectroscopic thin film thickness measurement system for semiconductor industries," Proceedings of Instrumentation and Measurement Technology Conference, Hamamatsu, Japan, ISBN: 0-7803-1880-3, vol. 2, 677-682 (1994).
- [142] W. G. Zijlstra, A. Buursma and W.P. Meeuwsen-van der Roest, "Absorption Spectra of Human Fetal and Adult Oxyhemoglobin, De-oxyhemoglobin, Carboxyhemoglobin and Methemoglobin," *Clinical Chemistry* 37, 1633-1638 (1991).
- [143] C. Franzini, G. Cattozzo and A. Pagani, "Serum Hemoglobin Measurement by Second Derivative Spectroscopy," *Int. Lab.*, October, 33-39 (1988).
- [144] M. L. Shih, W.D. Korte, C.R. Clark, "Multicomponent Spectroscopic Assay for Hemoglobin and Ferrihemoglobin Species in Methemoglobin Treatment of Cyanide Poisoning," *J. Anal. Toxicol.* 21(7), 543-547 (1997).
- [145] C. V. Sapan, R. L. Lundblad and N. C. Price, "Colorimetric Protein Assay Techniques," *Biotechnol. Appl. Biochem.* 29(2), 99-108 (1999).
- [146] M. M. Bradford, "A Rapid and Sensitive Method for the Quantitation of Microgram Quantities of Protein Utilizing the Principle of Protein-Dye Binding," *Anal. Biochem.* 72, 248-254 (1976).
- [147] A. G. Gornall, C. S. Bardawill and M. M. David, "Determination of Serum Proteins by Means of Biuret Reaction," *J. Biol.Chem.* 177, 751 (1949).
- [148] Z. Cui, "Nanofabrication: principles, capabilities and limits," Springer, ISBN-10:1441945369, pp.204 (2008) .

Part II

Development of microfluidic system
and optical tweezers for
electrophysiological investigations
of an individual cell

Authors:

Ahmed Alrifaiy, Nazanin Bitaraf, Olof Lindahl and Kerstin Ramser

Reformatted version of paper originally published in:

SPIE, the International Society for Optical Engineering.

©

Development of Microfluidic System and Optical Tweezers for electrophysiological investigations of an individual cell

A. Alrifaiy, N. Bitaraf, O. Lindahl and K. Ramser

Dept. of Computer Science and Electrical Engineering, Luleå University of Technology/Luleå tekniska universitet, 97187 Luleå, Sweden

ABSTRACT

We present a new approach of combining Lab-on-a-chip technologies with optical manipulation technique for accurate investigations in the field of cell biology. A general concept was to develop and combine different methods to perform advanced electrophysiological investigations of an individual living cell under optimal control of the surrounding environment. The conventional patch clamp technique was customized by modifying the open system with a gas-tight multifunctional microfluidics system and optical trapping technique (optical tweezers).

The system offers possibilities to measure the electrical signaling and activity of the neuron under optimum conditions of hypoxia and anoxia while the oxygenation state is controlled optically by means of a spectroscopic technique. A cell-based microfluidics system with an integrated patch clamp pipette was developed successfully. Selectively, an individual neuron is manipulated within the microchannels of the microfluidic system under a sufficient control of the environment. Experiments were performed to manipulate single yeast cell and red blood cell (RBC) optically through the microfluidics system toward an integrated patch clamp pipette. An absorption spectrum of a single RCB was recorded which showed that laser light did not impinge on the spectroscopic spectrum of light. This is promising for further development of a complete lab-on-a-chip system for patch clamp measurements.

Keywords: Optical Tweezers, neurons, microfluidics, patch clamp, hypoxia, anoxia and spectroscopy.

1. INTRODUCTION

The analyses of living cells using “Lab on a chip” has grown up to be an essential tool in the fields of cell biology as illustrated by the large number of publications in recent years. Microfluidic systems have shown unique advantages in investigative roles such as control of cell transport, immobilization, and manipulation of biological molecules and cells, as well as separation and mixing of chemical reagents^{1,2}. This enables an advanced analysis of intracellular investigations on a single-cell level.

Furthermore, combining microfluidic systems³ with optical manipulation techniques^{4,5} have emerged as powerful tool in various applications, especially the great impact on the ongoing revolution in of cell biology and biotechnology^{6,7}. As a result, several studies relating to single cell manipulation in environment-controlled microfluidics system for biological cell analysis have been published during the past few years^{8,9,10}. Consequently, it is also valuable to apply this system for advanced electrophysiological investigations of single biological objects in a micro-level control of cell environments.

The background of the research is the need of developing tools to study the functional role of a new discovered oxygen-binding hemoprotein called neuroglobin (Ngb)¹¹ that is found mainly in some types of neurons. The protein has been shown to have a protective role against hypoxia-related damage in the brain such as at stroke^{12,13}. The localization and the chemical composition of the protein have been studied and identified^{14,15,16,17,18} while an enormous desire is to learn about the functional role of the protein *in vivo*, i.e., inside the biological cells and under hypoxic and anoxic physiological conditions. In addition, it is important to investigate how Ngb affect the electrophysiological signaling capacity of the neurons in various environments in real time in order to understand the protective role of Ngb in the brain¹⁹.

The main approach is to develop a sealed multifunctional microfluidic system combined with optical tweezers and traditional patch clamp method to register the electrophysiological activity of individual neurons while the surrounding environment was changed experimentally. This system offers the possibility to select, trap and manipulate a single

neuron through a microchannel system to record the neuronal activity related to ngb concentrations during hypoxia and anoxia while controlling the oxygenation state of neurons by means of optical spectroscopy.

2. MATERIALS AND METHODS

The technical approach in this study was to develop and combine several methods into a complete system. The idea was to select and steer single neurons by optical tweezers through the gas-tight microfluidic system towards a fixed patch clamp micropipette for electrophysiological measurements. Optical spectroscopic measurements will simultaneously measure the oxygenation state of the hemoprotein that is exposed to changing oxygen conditions. The materials and methods used in our experimental work are presented briefly below.

2.1 Patch clamp technique

Patch clamp²⁰ is a well described technique to measure and analyze the electrophysiological activity of an individual biological cell under variable surroundings by recording the capacity of the tiny electrical signal across the ion channels in plasma membrane of the cell²¹. A solution-filled glass micropipette with an opening of one micrometer is moved slowly with a micromanipulator to attach the membrane of the cell located in the bottom of an open Petri-dish. An experimental giga “seal”²² giga-ohm resistance is build up between the membrane of the cell and the micropipette by means of negative pressure allowing a high-resolution registering of the electrical signal. The recording is performed through a recording electrode inside the patch clamp pipette and another reference electrode located in contact with the cell's immediate environment which is varied experimentally by a perfusion system (Fig. 1).

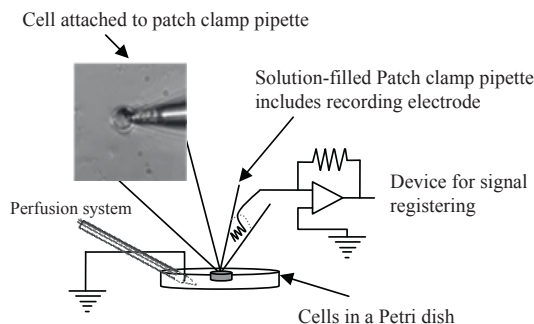


Figure 1: The principle of patch clamp.

An observable problem with the patch-clamp technique is to obtain stable giga-seals. The configuration of the giga ohm seal may change depending on which types of cell are investigated. It is determined by the surface properties of the tip, cellular properties such as cleanliness or effectiveness and mainly depend on the large extend of experience and patience of the researcher to perform a complete investigation. Patch-clamp setup's sensitivity to the vibrations requires a careful micro positioning of the pipette which may make the patch-clamp technique very time-consuming and labor-intensive. The resulting very low experimental throughput (i.e., few cells measured per day by one operator) limits the possibilities to exploit the high information of the cell under the whole investigation.

An observable problem with the patch-clamp technique is to obtain stable giga-seals. The configuration of the giga ohm seal may change depending on which types of cell are investigated. It is determined by the surface properties of the tip, cellular properties such as cleanliness or effectiveness and mainly depend on the large extend of experience and patience of the researcher to perform a complete investigation. Patch-clamp setup's sensitivity to the vibrations requires a careful micro positioning of the pipette which may make the patch-clamp technique very time-consuming and labor-intensive. The resulting very low experimental throughput (i.e., few cells measured per day by one operator) limits the possibilities to exploit the high information of the cell under the whole investigation.

Additionally, for our point of research, this open system cannot assemble the requirements of electrophysiological investigations in sufficient control of the oxygen content surrounding the neuron. Therefore, new approaches allowing higher throughput have been developed by modifying and replacing the open system with a sealed multifunctional microfluidic system and optical manipulation capabilities. The concept is to replace the traditional way of moving the patch clamp micropipette toward a cell laying in open system, by applying the optical tweezers to select, trap and steer the single cell to be moved through the microchannels towards a fixed, molded micropipette within the microfluidic system. The environment surrounding the neuron is changed by applying flows of solutions with varying oxygen levels through the microfluidic system.

2.2 Optical Techniques

Optical tweezers have been used to manipulate biological cell with high 3D-precision and without mechanical contact. To achieve strong optical trap, a near infrared laser beam is first expanded and thereafter highly focused by a microscope objective having a high numerical aperture (NA) onto the sample.

The theoretical approach of the optical manipulation technique has been investigated widely, therefore we present only the experimental configuration of the optical tweezers related to our setup.

The construction of the optical tweezers was achieved by using an IR- diode laser, operated at wavelength $\lambda = 830\text{nm}$, and power $P = 150\text{ mW}$ (Lasiris, StockerYale, USA). The laser was mounted on a commercial inverted optical microscope (IX 71, Olympus, Japan) built on a vibration-isolated table (Technical Manufacturing Corporation, TMC, USA) to minimize the noise due to vibrations. The wavelength of the laser was chosen to minimize heating of the sample and to avoid the photodamage, since biological samples have minimal absorption in the near infrared wavelength²³.

The beam of the laser light was expanded by two convex positive lenses, $f_1 = 25\text{ mm}$, $f_2 = 5\text{mm}$ and then guided through a system of mirrors (Thorlabs, Sweden) into the microscope to overfill the back focal plane of the objective (100X 1.4 NA, oil immersion; Olympus) to obtain a maximum of the trap stiffness. The laser light passed through a dichroic mirror (750-dcspxr, Chroma, USA) and focused strongly through the objective on the sample. The dichroic is chosen to give maximum reflectance of the trapping laser light into the objective and at the same time allowing transmission of the detection laser and visible light for the imaging.

Precise movement of the sample with respect to the laser tweezers was achieved by using an integrated nanometer precision translation stage (Olympus, Japan). Simultaneously, the oxygenation state of the cell in our setup was monitored by integrating an optical spectroscopic technique. A high-resolution optical UV-Vis spectrometer (Ocean Optics, HR4000, USA) was included in which light passing through the sample was captured through an optical fiber (Fig.2).

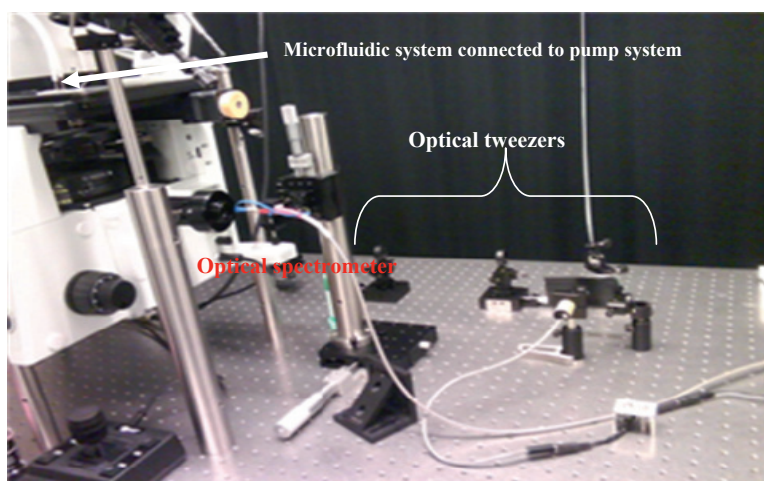


Figure 2: Optical tweezers and optical spectrometer integrated with an inverted microscope, mounted on vibration-free optical table.

2.3 Microfluidic system

The field of microfluidics deals with behavior, precise control and manipulation of fluids in systems associated with a micro-sized volume and low-energy consumption for applications in medical, biological and chemical sciences²⁴. This field of research interconnects many different fields such as engineering, physics, and biotechnology. The general applications are many such as inkjet print heads, DNA chips, micro-propulsion, micro-thermal technologies and lab-on-a-chip technology. Among the variety of techniques employed for the construction of microfluidic channels, we used the photolithographic technique^{25,26} to manufacture the silicon master and the soft lithographic technique²⁷ to create the microfluidics channels in PDMS polymer substrate.

The manufacturing process of a microfluidics system requires usually special clean room facilities; however we have made a lab-build setup to offer sufficient conditions of the manufacturing process.

The manufacturing procedure of microfluidics system started by CAD-drawing design for the desired microfluidic channel pattern and transferred on a plastic film by a commercial photographic technique to form a high resolution mask. Master design initiated by spin-coating of a silicon substrate with a negative photo-resist, SU-8 (MICRO CHEM, MA, USA) that then exposed to UV light through the high-resolution mask. After baking, a chemical bath development was used to remove the unexposed layer of SU-8 and the remaining pattern was appeared as positive microfluidics channels on the silicon wafer (Master).

It was preferred to integrate the patch-clamp micropipette within the microfluidic system by positioning the micropipette on a desired positive channel on the master before pouring PDMS to avoid the sealing damaging the tip of the pipette. Experimentally, a metal needle having similar dimensions as the patch-clamp pipette was put in contact with the desired positive microchannel on the silicon wafer (Master) that placed in a special designed cylinder-shaped holder operated as a mould for the fabrication of the PDMS (Fig. 4a). The holder was manufactured by computer numerical control (CNC) from polymethylmethacrylate (PMMA)²⁸, a simple machined plastic material with excellence surface properties that support easily the peeling off of the cross linked PDMS. The holder designed with 36 cylindrical 1.5 diameters holes spaced over the extern cylindrical area. The holes were pointed to a different positions on the master corresponds to the mould depth. This special holder enabled a highly precise positioning of the needle tip on a desired point (channel were cell was investigated) on the rotatable silicon master.

PDMS, Polydimethylsiloxane²⁹ have been used as a flexible elastic polymer in biological and medical applications mainly due to the advantages of biocompatibility, low toxicity, thermal stability, optical transparency, low-permeability to water and the ease of fabrication.

PDMS and its curing agent (Daw corning, Sylgard 184) were weight mixed according to a specific mixing-ratio of 10:1, and based on the desired stiffness. Thereafter, the mixture was degassed by vacuum desiccators at room temperature for 40 minutes in order to eliminate the air bubbles and to enhance the mixing. The PDMS was then poured onto the master inside the holder and cured.

The experimental work started with the integration of patch-clamp pipette with a tip diameter of 1 micron in the microfluidic channel system with the dimension of 20 μ m. The experiment succeeded by first making a model. A pipette-like metal needle passed through the cylindrical hole of the holder and another channel of PEEK tubing (JRT6004, Scantec, Sweden) in a contact with the desired positive microchannel on the silicon wafer in the holder. The PDMS was then poured onto the master in the cylinder holder and cured in room temperature for 2 hours and followed by a convection oven for 3 hour at 70 °C (Fig. 3a). The metal needle was then removed and the hardened PDMS was peeled off from the silicon master and the mould. Finally the patch-clamp pipette was carefully inserted through the PEEK channel so that the micro tip was intact in the microchannel without any damages.

The final PDMS block, i.e, the microfluidic system with an integrated patch clamp pipette was then bonded on a cover glass to seal the channel system with optical access and placed under an inverted microscope with an integrated optical tweezers (Fig. 3b). In addition, a programmable pump system (neMESYS, Cetoni, Germany) was connected to the microfluidic system for injection of the cells and variation of the cell's surrounded environment. A cell was trapped and manipulated by the optical tweezers through the microfluidic system toward the patch clamp pipette and an optical spectroscopic measurement was performed while cell environment was varied by the pump system.

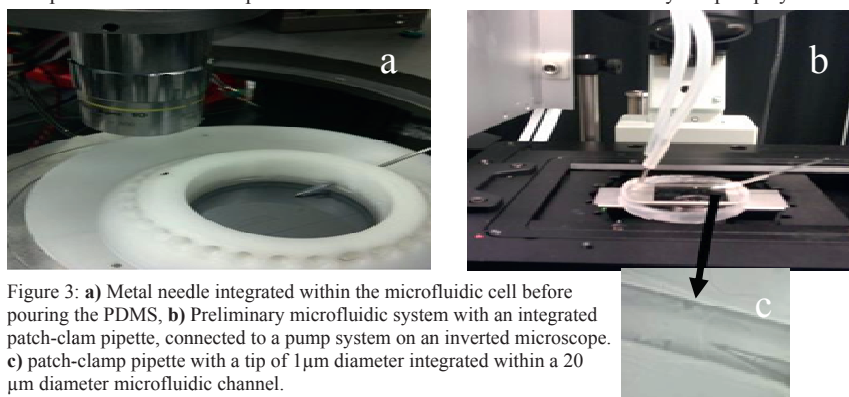


Figure 3: **a)** Metal needle integrated within the microfluidic cell before pouring the PDMS, **b)** Preliminary microfluidic system with an integrated patch-clamp pipette, connected to a pump system on an inverted microscope. **c)** patch-clamp pipette with a tip of 1 μ m diameter integrated within a 20 μ m diameter microfluidic channel.

4. EXPERIMENTAL RESULTS

Experiments were done to create a macro-micro connection between the developed multifunctional microfluidic system and the pump system for the inserting of the cells into the microfluidics system and environment's variation. Then, a single RBC was selected and trapped and manipulated within the microfluidic channel system toward the integrated patch clamp pipette. The trapping dynamics was recorded in real time with CCD camera integrated within the inverted microscope while the absorption spectrum of a trapped single RBC in contact with patch clamp pipette was registered (Fig. 4).

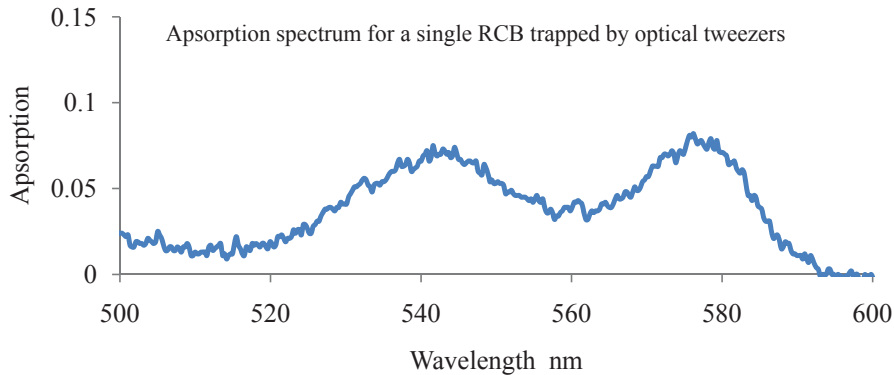


Figure 4: Absorption spectrum of a single red blood cell trapped by optical tweezers and in contact with a patch clamp pipette, inside the microfluidic system.

Preliminary measurements of electrophysiological activity on Medial Preoptic Neurons (MPN) med traditional patch-clamp without using microfluidics system have been performed successfully. Neurons, transported by a gravity-fed perfusion fluid flow system, showed similar reaction to hypoxia compared to neurons dissociated and left to settle on the bottom of the Petri-dish. One drawback with perfusion transported neurons was that the viability was diminished and they experienced necrosis faster than the dissociated neurons. However, this effect may be reduced by enhanced control of the fluid flow profile and by using shorter transport path, i.e., shorter tubings and connection to reduce the stress of the neurons caused by perfusion.

5. DISCUSSION AND FUTURE OUTLOOK

For practical reasons, the preliminary experimental work was performed with yeast and red blood cells. The development is ongoing to achieve a complete experimental setup with multifunctional microfluidic system. This system will allow the introduction of neurons from the preparation process through the pump system into the microfluidic system, in which a chosen neuron will be captured by optical tweezers and guided towards the channel where the pipette is integrated to perform electrophysiological experiments while the cell's environment changed experimentally. The advantage is to keep using the traditional patch clamp technique for measurement in a controllable environment with high efficiency in electrophysiological measurements and avoiding new expensive equipments. The ambition of the research is to develop a multifunctional mini-laboratory "lab on a chip" that will fit under microscope for detailed medical studies (Fig. 5).

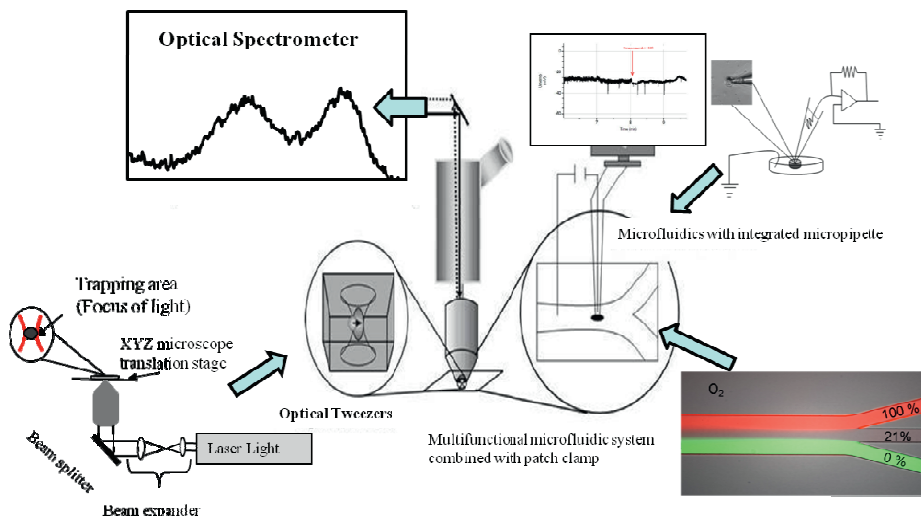


Figure 5: Schematic figure for the multifunctional system with patch clamp, optical tweezers, optical spectroscopy and microfluidic system.

6. ACKNOWLEDGEMENTS

The research is supported by grants from Objective 2, Norra Norrland-EU Structural fund and the Swedish Research Council.

REFERENCES

1. Wang, W., Liu, Y., Sonek, G. J., Berns, M. W., and Keller, R. A., "Optical trapping and fluorescence detection in laminar flow streams," *Appl. Phys. Lett.*, 67(8), 1057-1059 (1995).
2. Umehara, S., Wakamoto, Y., Inoue, I. and Yasuda, K., "On-chip single-cell microcultivation assay for monitoring environmental effects on isolated cells," *Res. Commun.* 305, 534-540 (2003).
3. Bruus, H., "Theoretical microfluidics", Oxford University press Inc., New York, USA (2006).
4. Lang, M. J. and Block, S. M., "Laser-based optical tweezers," *Am. J. Phys.* 71, 201-215 (2003).
5. Ashkin, A., "Optical trapping and manipulation of neutral particles using lasers," *Proc. Natl. Acad. Sci.* 94, 4853-4860 (1997).
6. Wibke Hellmich, W., Pelargus, C., Leffhalm, K., Ros, A. and Anselmetti, D., "Single cell manipulation, analytics, and label-free protein detection in microfluidic devices for systems nanobiology," *Electrophoresis* 26, 3689-3696 (2005).
7. Shelby, J.P., Mutch, S.A. and Chiu, D.T., "Direct manipulation and observation of the rotational motion of single optically trapped microparticles and biological cells in microvortices" *Anal. Chem.* 76, 2492-2497 (2004).
8. Ramser, K. and Hanstorp, D., "Optical manipulation for single-cell studies," *J. Biophoton.* 3(4), 187-206 (2010).
9. Voldman, J., Gray, M., Toner, M. and Schmidt, M., "A Microfabrication-based dynamic array cytometer," *Anal. Chem.* 74, 3984-3990 (2002).

10. Munce, N. R., Li, J., Herman, P. R. and Lilge, L., "Microfabricated system for parallel single-cell capillary electrophoresis", *Anal.Chem.*, 76(17), 4983-4989 (2004).
11. Burmester, T., Weich, B., Reinhardt, S. and Hankeln T., "A vertebrate globin expressed in the brain," *Nature* 407, 520-523 (2000).
12. Sun, Y., Jin, K., Mao, X. O., Zhu, Y. and Greenberg, D. A., "Neuroglobin is up-regulated by and protects neurons from hypoxic-ischemic injury" *PNAS*, 98(26), 15306-15311 (2001).
13. Li, R. C., Lee, S. K., Pouranfar, F., Brittian, K. R., Clair, H. B., Row, B. W., Wang, Y. and Gozal, D., "Hypoxia differentially regulates the expression of neuroglobin and cytoglobin in rat brain," *Brainresearch* 1096, 173-179 (2006).
14. Hankeln, T., Ebner, B., Fuchs, C., Gerlach, F., Haberkamp, M., Laufs, T. L., Roesner, A., Schmidt, M., Weich, B., Wystub, S., Saaler-Reinhardt, S., Reuss, S., Bolognesi, M., De Sanctis, D., Marden, M.C., Kiger, L., Moens, L., Dewilde, S., Nevo, E., Avivi, A., Weber, R.E., Fago, A. and Burmester, T., "Neuroglobin and cytoglobin in search of their role in vertebrate globin family," *J. Inorg. Biochem.* 99, 110-119 (2005).
15. Kriegl, J. M., Bhattacharyya, A. J., Nienhaus, K., Dang, P., Minkow, O. and Nienhaus, G. U., "Ligand binding and protein dynamics in neuroglobin," *Proc. Natl. Acad. Sci., USA*, 99, 7992-7997 (2002).
16. Schmidt, M., Giessler, A., Laufs, T., Hankeln, T., Wolfrum, U. and Burmester, T., "How Does the Eye Breathe? Evidence for neuroglobin-mediated oxygen supply in the mammalian retina," *J. Biol. Chem.* 278, 1932-1935 (2003).
17. Geuens, E., Brouns, I., Flamez, D., Dewilde, S., Timmermans, J. P. and Moens, L., "A globin in the nucleus," *J. Biol. Chem.* 278, 30417-30420 (2003).
18. Wystub, S., Laufs, T., Schmidt, M., Burmester, T., Maas, U., Saaler-Rienhardt S., Hankeln, T., and Reuss, S., "Localization of neuroglobin protein in the mouse brain," *Neurosci. Letts.* 346, 114-116 (2003).
19. Brunori, M. and Vallone, B., "Neuroglobin, seven years after," *Cell Mol. Life Sci.* 64, 1259-1268 (2007).
20. Lapointe, J. and Szabo, G., "A novel holder allowing internal perfusion of patch-clamp pipettes," *Pflügers Arch, J. of Physiology* 405(3), 285-293 (1985).
21. Sakmann, B. and Neher, E., "Patch Clamp Techniques for Studying Ionic Channels in Excitable Membranes," *Ann. Rev. of Phys.* 46, 455-472 (1984).
22. Avi, P., Ziv, G., Vincent, T. Moy, Y., Karl, L., Magleby, Y. and Shai, D. S., "Ionic Requirements for Membrane-Glass Adhesion and Giga Seal Formation in Patch-Clamp Recording," *Biophysical Journal* 92(11), 3893-3900, (2007).
23. Neuman, K. C., Chadd, E. H., Liou, G. F., Bergman, K. and Block, M., "Characterization of photodamage to *Escherichia coli* in optical traps," *Biophys. J.* 77, 2856-2863 (1999).
24. Enger, J., Goksör, M., Ramser, K., Hagberg, P. and Hanstorp, D., "Optical tweezers applied to a microfluidic system," *Lab Chip* 4(3), 196-200, (2004).
25. Chen, C. S., Mrksich, M., Huang, S., Whitesides, G. M., and Ingber, D. E., "Geometric control of cell life and death," *Science* 276, 1425-1428, (1997).
26. Singhvi, R., Kumar, A., Lopez, G., "Engineering cell shape and function," *Science* 264, 696-698, (1994).
27. Xia, Y. and Whiteside, G., "Soft lithography," *Ann. Rev. Mater. Sci.* 28, 153-184, (1998).
28. Kutz, M., "Handbook of Materials Selection," John Wiley & Sons., 341-342, ISBN 0471359246 (2002).
29. Kuncová, J. and Kallio, P., "PDMS and its suitability for analytical microfluidic devices," *Proc. IEEE, Eng. Med. Biol. Soc.* 1, 2486-2489 (2006).

How to integrate a micropipette
into a closed microfluidic system:
Absorption spectra of an optically
trapped erythrocyte

Authors:

Ahmed Alrifaiy and Kerstin Ramser

Reformatted version of paper originally published in:

OSA, Journal of biomedical optics express .

©

How to integrate a micropipette into a closed microfluidic system: absorption spectra of an optically trapped erythrocyte

Ahmed Alrifaiy^{1,2,*} and Kerstin Ramser^{1,2}

¹Department of Computer Science, Electrical and Space engineering, Luleå University of Technology, SE-971 87 Luleå, Sweden

²Centre for Biomedical Engineering and Physics, Luleå University of Technology and Umeå University, Luleå and Umeå, Sweden

*ahmed.alrifaiy@ltu.se

Abstract: We present a new concept of integrating a micropipette within a closed microfluidic system equipped with optical tweezers and a UV-Vis spectrometer. A single red blood cell (RBC) was optically trapped and steered in three dimensions towards a micropipette that was integrated in the microfluidic system. Different oxygenation states of the RBC, triggered by altering the oxygen content in the microchannels through a pump system, were optically monitored by a UV-Vis spectrometer. The built setup is aimed to act as a multifunctional system where the biochemical content and the electrophysiological reaction of a single cell can be monitored simultaneously. The system can be used for other applications like single cell sorting, in vitro fertilization or electrophysiological experiments with precise environmental control of the gas-, and chemical content.

©2011 Optical Society of America

OCIS codes: (350.4855) Optical tweezers or optical manipulation; (170.3880) Medical and biological imaging; (300.1030) Absorption; (280.2490) Flow diagnostics; (220.4000) Microstructure fabrication; (110.0180) Microscopy.

References and links

1. A. Ashkin, J. M. Dziedzic, and T. Yamane, "Optical trapping and manipulation of single cells using infrared laser beams," *Nature* **330**(6150), 769–771 (1987).
2. T. M. Squires and S. R. Quake, "Microfluidics: Fluid physics at the nanoliter scale," *Rev. Mod. Phys.* **77**(3), 977–1026 (2005).
3. W. W. Hellmich, C. Pelargus, K. Leffhalm, A. Ros, and D. Anselmetti, "Single cell manipulation, analytics, and label-free protein detection in microfluidic devices for systems nanobiology," *Electrophoresis* **26**(19), 3689–3696 (2005).
4. S. Chu, J. E. Bjorkholm, A. Ashkin, and A. Cable, "Experimental observation of optically trapped atoms," *Phys. Rev. Lett.* **57**(3), 314–317 (1986).
5. A. Ashkin, K. Schütze, J. M. Dziedzic, U. Euteneuer, and M. Schliwa, "Force generation of organelle transport measured in vivo by an infrared laser trap," *Nature* **348**(6299), 346–348 (1990).
6. J. Yang, Y. Huang, X. B. Wang, F. F. Becker, and P. R. C. Gascoyne, "Cell separation on microfabricated electrodes using dielectrophoretic/gravitational field-flow fractionation," *Anal. Chem.* **71**(5), 911–918 (1999).
7. I. K. Glasgow, H. C. Zeringue, D. J. Beebe, S. J. Choi, J. T. Lyman, N. G. Chan, and M. B. Wheeler, "Handling individual mammalian embryos using microfluidics," *IEEE Trans. Biomed. Eng.* **48**(5), 570–578 (2001).
8. D. Figeys, S. P. Gygi, G. McKinnon, and R. Aebersold, "An integrated microfluidics-tandem mass spectrometry system for automated protein analysis," *Anal. Chem.* **70**(18), 3728–3734 (1998).
9. Z. H. Fan, S. Mangru, R. Granzow, P. Heaney, W. Ho, Q. Dong, and R. Kumar, "Dynamic DNA hybridization on a chip using paramagnetic beads," *Anal. Chem.* **71**(21), 4851–4859 (1999).
10. D. D. Cunningham, "Fluidics and sample handling in clinical chemical analysis," *Anal. Chim. Acta* **429**(1), 1–18 (2001).
11. F. S. Ligler, "Perspective on optical biosensors and integrated sensor systems," *Anal. Chem.* **81**(2), 519–526 (2009).
12. B. H. Weigl, R. L. Bardell, and C. R. Cabrera, "Lab-on-a-chip for drug development," *Adv. Drug Deliv. Rev.* **55**(3), 349–377 (2003).

13. L. Yao, B. Liu, T. Chen, S. Liu, and T. Zuo, "Micro flow-through PCR in a PMMA chip fabricated by KrF excimer laser," *Biomed. Microdevices* **7**(3), 253–257 (2005).
14. M. J. Madou, *Fundamentals of Microfabrication: The Science of Miniaturization*, 2nd ed. (CRC Press, 2002).
15. Y. Xia and G. M. Whitesides, "Soft lithography," *Annu. Rev. Mater. Sci.* **28**(1), 153–184 (1998).
16. P. Abgrall, L. N. Low, and N. T. Nguyen, "Fabrication of planar nanofluidic channels in a thermoplastic by hot-embossing and thermal bonding," *Lab Chip* **7**(4), 520–522 (2007).
17. S. Balslev, A. M. Jorgensen, B. Bilenberg, K. B. Mogensen, D. Snakenborg, O. Geschke, J. P. Kutter, and A. Kristensen, "Lab-on-a-chip with integrated optical transducers," *Lab Chip* **6**(2), 213–217 (2006).
18. H. Qi, X. Wang, T. Chen, X. Ma, and T. Zuo, "Fabrication and characterization of a polymethyl methacrylate continuous-flow PCR microfluidic chip using CO₂ laser ablation," *Microsyst. Technol.* **15**(7), 1027–1030 (2009).
19. P. Liuni, T. Rob, and D. J. Wilson, "A microfluidic reactor for rapid, low-pressure proteolysis with on-chip electrospray ionization," *Rapid Commun. Mass Spectrom.* **24**(3), 315–320 (2010).
20. G. B. Lee, S. H. Chen, G. R. Huang, W. C. Sung, and Y. H. Lin, "Microfabricated plastic chips by hot embossing methods and their applications for DNA separation and detection," *Sens. Actuators B Chem.* **75**(1-2), 142–148 (2001).
21. O. Loh, R. Lam, M. Chen, N. Moldovan, H. Huang, D. Ho, and H. D. Espinosa, "Nanofountain-probe-based high-resolution patterning and single-cell injection of functionalized nanodiamonds," *Small* **5**(14), 1667–1674 (2009).
22. N. A. Kotov, J. O. Winter, I. P. Clements, E. Jan, B. P. Timko, S. Campidelli, S. Pathak, A. Mazzatenta, C. M. Lieber, M. Prato, R. V. Bellamkonda, G. A. Silva, N. W. S. Kam, F. Patolsky, and L. Ballerini, "Nanomaterials for Neural Interfaces," *Adv. Mater. (Deerfield Beach Fla.)* **21**(40), 3970–4004 (2009).
23. K. Ramser and D. Hanstorp, "Optical manipulation for single-cell studies," *J Biophotonics* **3**(4), 187–206 (2010).
24. K. Schütze, H. Pösl, and G. Lahr, "Laser micromanipulation systems as universal tools in cellular and molecular biology and in medicine," *Cell. Mol. Biol. (Noisy-le-grand)* **44**(5), 735–746 (1998).
25. A. Ashkin and J. M. Dziedzic, "Optical trapping and manipulation of viruses and bacteria," *Science* **235**(4795), 1517–1520 (1987).
26. K. Kim, S. Kang, K. Matsumoto, and H. Minamitani, "Thin film waveguide sensor for measurement of the absorption coefficient of hemoglobin derivatives," *Opt. Rev.* **5**(4), 257–261 (1998).

1. Introduction

The development of new approaches to investigate mechanisms in living cells under in vivo like conditions is of highest importance. Desirably, measurements should be carried out under well-controlled physiological conditions, i.e. different oxygen levels and addition/removal of biochemical substances or nutrients. Many single cell studies are hitherto carried out on microscopes where they are studied by optical techniques such as optical spectroscopy, patch-clamp-, and time resolved techniques. Recently, much attention has been paid to functional systems that include optical tweezers [1] and microfluidic system [2]. These systems have released innovative approaches for basic and applied research for diverse biological studies of single cells [3].

Optical tweezers, an increasingly important tool in biophysics and cell biology, utilize light to trap and manipulate small particle in three dimensions. In a typical setup of optical tweezers, a stable trap is achieved by a strongly focused laser beam through a high-numerical aperture (NA) microscope objective. The phenomenon of using the momentum of light to manipulate particles was first experimentally demonstrated on atoms [4]. Shortly thereafter biological cells were manipulated using infrared lasers [5]. The optical tweezers are widely used in many applications like cell transport and separation [6], manipulation of biological cells [7], sample cell analysis by mass spectrometry [8], DNA analysis [9] and other applications for clinical diagnostics [10].

Microfluidic systems typically consist of a structure of channels with diameters ranging between 10 and 1000 μm with a $\mu\text{l/s}$ flow of solvents. They can easily be designed individually for each experiment and have proven to give unsurpassed control over the flow and thus enable fast environmental changes [11,12]. One benefit of the systems is that they can be made of transparent materials such as rubber silica, Plexiglas or glass and as a consequence they can easily be implemented onto microscopes to be combined with suitable read-out techniques. Especially Plexiglas PMMA (Poly-methyl methacrylate) microchips have gained popularity in various biological and medical applications [13]. They are less expensive than glass microchips [14] and the complex development process of the lithographical

microchips can be avoided [15]. The main advantage of using PMMA based microfluidic chamber is the impermeability to air, gases and other properties like low toxicity, optical transparency, thermal stability and they are easy to manufacture [16]. They have been applied to produce micro-mixers [17], polymerase chain reaction microchips (PCR) [18], microfluidic reactors [19] and capillary electrophoresis microchips (CE) [20].

Recently, many new concepts of nanofluidic delivery platforms, including integrated nanofluidic probes, have been developed. For instance, the so called Nanofountain probe (NFP) [21] is a new promising technique based on Dip-Pen Nanolithography (DPN). These nanofluidic probes consist of nano-channels which are used for direct nanoliter-delivery of specific bioactive solutions through a conical tip with a nano-pore attached with sub-cellular precision to a single cell while the cellular response can be imaged simultaneously. However, the impact of the nano-probes breaking the membrane of the cell, the biocompatibility of the nanomaterials, and the impact of bio-electronic integration need further investigations before the technique can be applied for electrophysiological studies [22]. Despite of the promising prospect of the NFPs, the patch clamp technique combined with microfluidic microchips that incorporate microfluidic channels, micro pumps and micro valves are well established alternatives that can be employed directly.

The so called lab-on-a-chips facilitate a variety of biological applications. The significant benefits are that minimal amount of reagents and analytes are used and that they can function as portable clinical diagnostic devices, i.e. time-consuming laboratory analysis procedures can be reduced. The great impact of these systems is shown in studies of manipulated biological cells in environment-controlled analytical systems [23,24].

Despite of all the progresses that have been achieved by combining optical tweezers with microfluidic systems one great challenge has, to our knowledge, not been conquered yet. How can a micro-pipette be integrated within a closed movable system? In many applications such as cell sorting, in-vitro fertilization or patch-clamp experiments the biological cell has to be brought in close contact to a micro-pipette. Usually a precise and electronically steered 3D manipulation device is moved towards the cell under an open space on the microscope. Hence the possibility of applying closed microfluidic technique is unfeasible. Here we demonstrate a new concept. By integrating optical tweezers, the cell can be steered in 3D towards the micropipette that is integrated in the microfluidic system.

The fabrication of the microfluidic chamber presented here bases on PMMA, and is performed by a CNC (Computer Numerical Control) Circuit Board milling machine. A patch clamp micropipette was included within the gastight microfluidic chamber. To prove the principle, a single RBC was optically trapped and manipulated within the microchannels towards the integrated micropipette. The UV-Vis absorption spectra in the oxy and deoxy-state of the RBC were acquired under controlled conditions created by the micro flow. The experimental work presents a microfluidic chamber with an integrated micropipette combined with optical tweezers and optical spectroscopy that acts as multifunctional system for various biomedical and electrophysiological applications with complete environmental control.

2. Material and Methods

The main parts of the experimental setup, as seen in Fig. 1, are mounted on an inverted optical microscope (IX 71, Olympus, Japan) placed on a vibration-isolated table (Technical Manufacturing Corporation, TMC, USA). The techniques used in this work are presented below.

Preparation of RBC and Solutions

Fresh RBCs were prepared from blood taken from a healthy volunteer. 0.05 ml blood was diluted in 2 ml solution of Phosphate-Buffered Saline (PBS), pH 7.4, temperature 23°C. The oxygen-free solution was prepared by 20mg Natriumdithionit, $\text{Na}_2\text{O}_4\text{S}_2$ (Sigma-Aldrich,

USA), dissolved in 4ml (PBS) solution. The solutions were prepared in Petri dishes and sucked into the gastight syringes of the pump system.

Optical Trapping of Single RBC

The optical tweezers build upon an IR-diode laser (IQ1A, Power Technology, USA), operating at 808nm with an average power of 200 mW. The wavelength of the laser was chosen to minimize heating and photodamage of the sample [25]. The laser beam was first expanded by two convex positive lenses of 50 and 250 mm, mounted on two XYZ-translation stages (Thorlabs, USA), and steered by mirrors (Thorlabs, USA) into the microscope. The laser beam was then guided to the objective throughout a dichroic mirror (750-dcspxr, Chroma Technology, USA). The expanded beam overfilled the back focal plane of the oil immersion objective (100x, 1.4 NA, Olympus, Japan) to obtain good trap stiffness. The trap stiffness was estimated qualitatively. Visual observations showed a strong and stable trap while the optically trapped red blood cells were exposed to a high flow rate of fluid (up to 20 μ l/s) through the channels and while imposing a force on the trapped cell by moving the stage.

The positioning of the optically trapped red blood cell was enabled by keeping the trapped cell still while moving the microfluidic chip including the micropipette mounted on the nanometer-precision XYZ translation stage of the microscope. This allowed the microfluidic chamber including the micropipette to move in micro-precision in 3 dimensions while the position of the optical trap was fixed and always positioned in the center of the field of view.

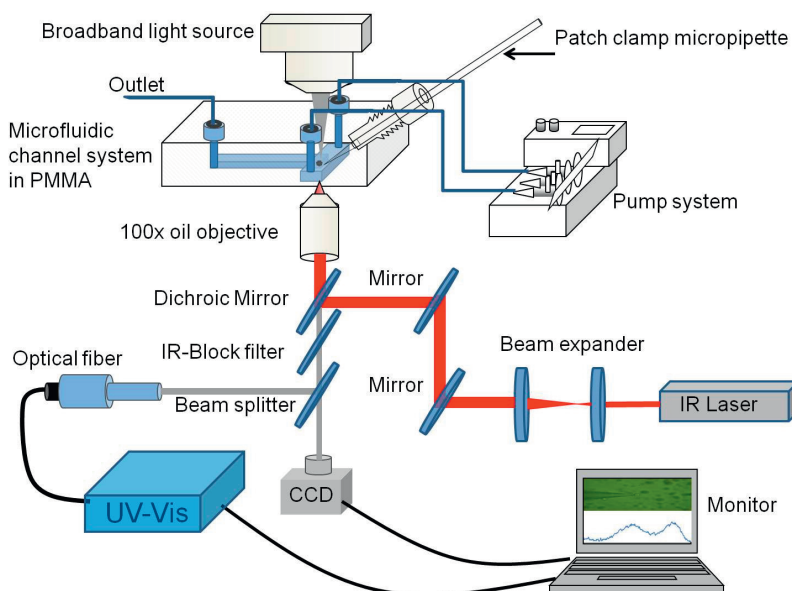


Fig. 1. Inverted microscope that incorporates the following techniques: Gastight lab-on-a-chip with an integrated micropipette coupled to a pump system, optical tweezers for 3D steering of the single cells comprising of an IR laser, a beam expander, mirrors and a dichroic mirror and an IR blocking filter to block the IR laser. UV-Vis spectrometer with an integrated optical fiber to record the oxygenation states of the RBC, CCD camera to monitor the trapping dynamics of the cells within the micro-channel system.

Optical Spectroscopy

The oxygenation state of a single optically trapped RBC was monitored by acquiring the absorption spectra by an UV-Vis spectrometer (Ocean Optics, HR4000, USA) in the following way: The visible light from the halogen lamp of the microscope illuminated the sample. The transmitted light that had passed through the sample was collected by the microscope objective and guided through the dichroic mirror. Thereafter it was divided by a beam-splitter to the CCD (20%) and to the optical fiber (80%) situated outside the right-hand side-port of the microscope. The optical fiber was connected to the UV-Vis spectrometer. The optical fiber, with a core size of diameter of 50 μm , was mounted on a 3D translation stage (Thorlabs USA). It was precisely aligned by moving the translation stage in the XYZ directions to guide the transmitted light from the microscope objective to the center of the fiber. The optical fiber facilitated the alignment of the optical path considerably and enabled the monitoring of the absorption spectrum of a single red blood cell.

To test the alignment of the spectrometer, a RBC within the microchannel was steered to the center of the field of view, Fig. 2(B) position 1, and an absorption spectrum was taken, Fig. 2(A). The spectrum shows the typical oxygenated state of the RBC with two maxima at 542 nm and 578 nm [26]. Thereafter, the center of the field of view of the microscope was positioned in a “RBC-free” environment, Fig. 2(B) position 2. A second absorption spectrum was taken to prove that no signals from RBCs were present, Fig. 2(C). The absorption spectra shown in this paper were binomially fitted by data-analyzing software program (Igor Pro).

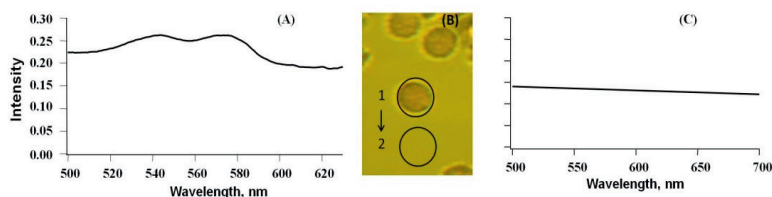


Fig. 2. (A) UV-Vis absorption oxygenation spectrum of the single RBC, (B) The center of the fiber was moved from position 1 (single RBC) to position 2 (cell-free zone), (C) UV-Vis absorption spectrum of the cell-free zone.

Microfluidic System

The manufacturing process of the closed microfluidic chamber was performed by a CNC Circuit Board milling Machine. The desired T-shaped microchannel were initially designed by a software program (QCAD) and transferred onto a slab of PMMA by the CNC machine. The channels were then sealed between two cover slips by an UV-curable adhesive material with low viscosity and high optical transparency (EPO-TEK OG603, Epoxy Technology, USA). It classified to USP Class VI biocompatibility standards that meet the requirements for medical application. The microfluidic chamber was equipped with two inlets and one outlet adjacent to the microchannels and connected by gas-tight PEEK tubing (ScanTec, Sweden) to the pump system (neMESYS, Cetoni, Germany). The pump system was used for the infusion of cells and solutions with varying oxygen content.

The procedure of integrating the patch clamp micropipette started by CNC drilling of a hole that extended at 45 degrees from the upper edge of the microfluidic chamber to the intersection zone within the T-shape microfluidic channel. The upper edge of the hole was threaded to fit a fine hollow screw (JR-5508-5, VICI Jour, Switzerland). The micropipette was inserted through the hollow screw and the drilled hole into the microfluidic chamber, while the tip of the pipette was monitored visually in the microfluidic channel. To ensure an airtight seal around the drilled hole, the diameter of the hole was fitted precisely to the outer diameter of the micropipette. Additionally, a gas-tight fitting (PEEK, JR-55003-5, VICI Jour,

Switzerland) was used to make an airtight seal between the hollow screw and the hole. The hollow screw was used to fine-position the tip of the micropipette to the RBC in the microchannel, as seen in Fig. 3(A) and 3(B).

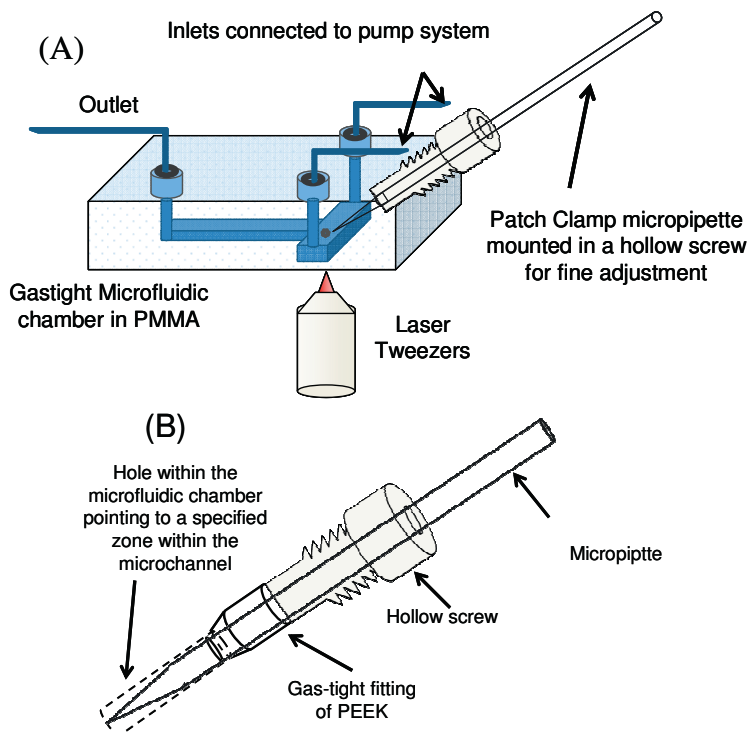


Fig. 3. (A) Schematic of the gastight microfluidic chamber including the patch clamp micropipette and inlets to be connected to a pump system. (B) The micropipette was fitted within the microfluidic chamber in a gastight surrounding.

3. Experimental Results and Discussions

The closed microfluidic chamber with the integrated micropipette was placed on the microscope stage and connected the pump system for latter insertion of RBCs and for the variation of the oxygenation state of the solution. The micropipette was carefully inserted through the hollow screw into the microfluidic chamber while the tip of the pipette entering the intersection-zone within the T-shape microfluidic channel was monitored visually. The cells were inserted to the microfluidic channel by the pump system in a low flow rate of $1 \mu\text{l/s}$. By the optical tweezers, a single RBC within the microchannel was optically trapped and steered through the microfluidic channel to the tip of the pipette. Simultaneously the trapping dynamics were recorded in real time with the CCD camera, see Fig. 4. The micropipette was then precisely adjusted by the hollow screw to attach to the membrane of the trapped cell.

The absorption spectra of the trapped cell were then acquired and monitored by the UV-Vis spectrometer under environmental variations by the pump system. Three absorption spectra of the trapped RBC in the oxy-, deoxy-, and oxy states were acquired as shown in Fig. 5.

At the beginning of the experiment ($t = 0$), the absorption spectrum was acquired in the oxygenated state, Fig. 5(A). The spectrum showed peaks at 540 nm and 576 nm, which is typical for the oxy-spectrum of red blood cells [21]. The trapped RBC was then deoxygenated by 1 minute exposure to the oxygen-free solution. After 59s, the absorption spectrum of the RBC was gradually transformed to the deoxygenated state, showing the typical peak at 560nm [21], see Fig. 5(B). The spectrum was transformed back to the oxygenated state after 21minutes, Fig. 5(C).

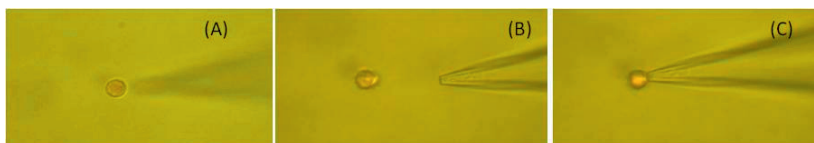


Fig. 4. (A) Single optically trapped RBC, here the micropipette is situated above the RBC, (B) RBC in the same optical plane as the micropipette. (B) The RBC in contact with the patch clamp micropipette.

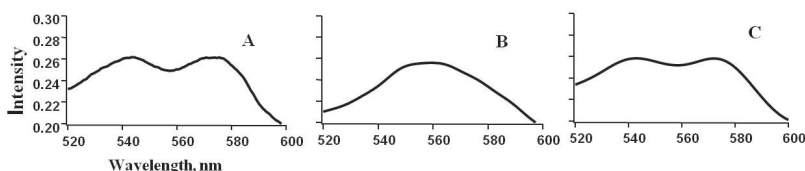


Fig. 5. Absorption spectra of the trapped RBC in contact with micropipette in the microfluidic system in (A) oxygenated state (B) deoxygenated state and (C) re-oxygenated state.

The microfluidic chamber was designed to perform electrophysiological investigations of single cells with reliable control of the environment. The presented microfluidic chamber can be modified for various electrophysiological techniques. Using CNC circuit board machines to design and create the microfluidic channel on various materials is beneficial due to the low cost and the high efficiency.

A number of improvements will be carried out on the presented prototype. The microfluidic channels will be coated with UV curable epoxy to create an optical transparency similar to glass microchips. The fine screw that is used to integrate the micropipette will be replaced with a build-in tiny 3D micromanipulator. The process of transporting the cell through the pump system to the microfluidic chamber will be replaced by a new design where the cell will be prepared directly in the microfluidic chamber. The cells will be transported to the microchannel by applying a negative pressure through developed micro valves. This is to minimize the stress that the cells experience during transport through long tubing and to ensure that the cells will not stick onto the inner wall of the tubing.

4. Conclusions

Hereby we have presented a new way of integrating a micro-pipette into a closed microfluidic system with an integrated micro-pipette. The closed lab-on-a-chip offers the possibility to analyze individual cells under environmental control with a minimum of oxygen-diffusion into the microchannels during the measurements. As a proof of principle, the oxygenation sequence of a single RBC was studied at the tip of the integrated patch clamp micropipette.

The microfluidic chamber was designed to act as a multifunctional system for simultaneous and high-throughput experiments. The future aim is to perform patch clamp experiments for electrophysiological investigations while simultaneously monitoring the biochemical composition of the sample by optical spectroscopy. The simplicity and stability of the microfluidic system has excellent potential to enable high volume production of

scalable microchips for various biomedical applications. The subsequently ambition is to use this system as a mini laboratory that has benefits in cell sorting, pharmaceutical, patch clamp, and fertilization experiments where the gaseous and the biochemical content is of importance.

Acknowledgments

This work was supported by EU Structural fund, Objective 2, Norra Norrland, the Swedish Research Council, and the Kempe Foundation. The authors would like to thank Dr. Johan Borg and Mikael Larsson at Luleå University of Technology for valuable input.

Hypoxia on a chip - a novel
approach for patch-clamp in a
microfluidic system with full
oxygen control

Authors:

Ahmed Alrifaiy, Nazanin Bitaraf, Olof Lindahl and Kerstin Ramser

Reformatted version of paper submitted to:

World Congress on Medical Physics and Biomedical Engineering.

©

Hypoxia on a chip—a novel approach for patch-clamp in a microfluidic system with full oxygen control

A. Alrifaiy^{1,3}, N. Bitaraf^{1,3}, M. Druzin², O. Lindahl^{1,3} and K. Ramser^{1,3}

¹Department of Computer Science, Electrical and Space Engineering, Luleå University of Technology, SE-971 87, Luleå, Sweden

²Department of Integrative Medical Biology, Section for Physiology, Umeå University, SE-901 87 Umeå, Sweden

³CMTF, Centre for Biomedical Engineering and Physics, Luleå University of Technology and Umeå University, Luleå and Umeå, Sweden

Abstract—Here a new approach to perform patch-clamp investigations under anoxic and normoxic conditions on nerve cells from Sprague Dawley rats is presented. A patch-clamp micropipette is integrated within a poly-methyl methacrylate (PMMA) based microchip giving optimal control over the oxygen content and the biochemical environment. Nerve cells were trapped by optical tweezers and steered towards the patch-clamp micropipette within the micro-channels. Several experiments were performed to show proof of principle. The oxygen content within the microfluidic chamber was measured to 0.5–1.5 %. The photo-induced effect of the optical tweezers on the nerve cells was investigated in an open Petri dish. The optical trapping did not influence measurements. The microfluidic system was further tested in patch-clamp experiments. This approach showed significant advantages regarding the tuning of the oxygen content and may be used in various electrophysiological investigations of single cells demanding optimal control of the surroundings.

Keywords—Patch-clamp, optical tweezers and lab-on-a-chip.

1. INTRODUCTION

According to the World Health Organization (WHO) stroke is the second common cause of death and disability in the western world. Resulting brain damage is caused by a shortage of the oxygen delivery to nerve cells. It is important to gain a fundamental understanding on how the lack of oxygen in brain tissue activates intrinsic bio-molecular defense mechanisms which reduce brain damages due to stroke.

The discovery of a new hemoprotein termed neuroglobin (Ngb) led to intense studies showing a protective, but yet unknown, function of the protein against hypoxia-related damage. Our long term aim is to learn more about this neuroprotective role by measuring the electrophysiological activity of nerve cells simultaneously with the surveillance of Ngb related action by means of optical spectroscopy.

The patch-clamp technique is routinely used to measure and analyze the electrophysiological activity of individual biological cells by means of the tight seal patch-clamp technique¹. Numerous studies have been performed where the

electrophysiological response of neurons, neuron-like cells, and myocytes upon oxygen deprivation was assessed with patch-clamp^{2, 16}.

The oxygen content varies under physiological conditions and is known to be very heterogeneous in various parts of the brain¹⁷. Precise control of the oxygen content during measurement is crucial for performance of accurate experiments which mimic the physiological environment of single nerve cells. Generally during experiments the reduction of oxygen in cell proximity is reached either by subjecting the cells to solutions with reduced oxygen content, i.e. hypoxic or anoxic solution^{2–13}, or with so-called chemical hypoxia or anoxia by inhibition of the electron transport chain in the mitochondrion with cyanide^{4–16}. Hypoxic or anoxic solutions are made by purging solutions with Ar, N₂, CO₂,^{2–13} or by addition of azides to the solution¹⁷. The oxygen content of the solutions which are used to perfuse sample cells to trigger oxygen deprivation varies from ~ 1.3 % (10 mmHg) to ~ 3.9% (30 mmHg) in different studies. The oxygen concentrations of solutions regarded as normoxic also varies from ~ 15 % (120 mmHg) to 80 % (608 mmHg).

Microfluidic systems, so called lab-on-a-chips, consist of micro sized channel systems prepared on transparent materials¹⁸. They enable precise control of the fluid flow to deliver quick environmental changes^{19, 20}. Lab-on-a-chips have recently been applied for studies on biological cells where several techniques were combined²¹. Microfluidic devices can be fabricated with a broad variety of technologies such as photolithography, soft lithography and CNC (Computer Numerical Control) micromachining. They are made out of different types of material such as PDMS (Polydimethylsiloxane), PMMA (Poly-methyl methacrylate) or glass, and can easily be combined with suitable read-out techniques on optical microscopes.

In many lab-on-a-chips it is necessary to control the location of individual cells in 3D within the micro-channel system. This has been achieved by optical tweezers²³, which provide excellent means to trap and manipulate the biological cells. Optical tweezers use light radiation forces to trap and steer small dielectric objects in three dimensions. Experimentally, a stable optical trap is achieved by focusing a laser beam strongly through a high-numerical aperture (NA)

microscope objective onto the sample. The trapped object is usually manipulated by moving the trap and/or the sample stage. Microfluidic systems combined with optical tweezers have been applied in various applications of single cell investigations²².

The combination of optical tweezers, lab-on-a-chips and patch-clamp could be desirable for many applications. For instance, the traditional patch-clamp measurements involves that a micropipette is steered in three dimensions to get in close contact to a biological cell. Consequently the possibility to patch a cell in a closed microfluidic system by the pipette is unfeasible without innovative design and modification.

In our experimental work, we developed a PMMA based closed microfluidic chip with an integrated patch-clamp micro-pipette where a biological cell was optically trapped and guided to the tip of the patch-clamp micropipette. The up-to date results showed the ability to form megaohm seal between the micropipette and the trapped nerve cell during rapid variation of environments within the closed micro-chip. The ongoing experiments are aimed to perform complete protocols of patch-clamp electrophysiological investigations on single nerve cells under variation of the environments.

II. MATERIALS AND METHODS

A. Preparation of neurons and solutions

Ethical approval of the procedures described was given by the regional ethics committees for animal research ("Umeå djurförsöksetiska nämnd", approval No. A13-08 and A18-11).

Nerve cells were prepared from the brains of Sprague Dawley rats (3-6 weeks old) that were decapitated without anesthetics. The brains were rapidly removed and placed in pre-oxygenated ice-cold (≤ 4 °C) incubation solution containing (in mM) 150 NaCl, 5 KCl, 2 CaCl₂ ($\times 2H_2O$), 10 HEPES, 10 glucose, 4.93 Trizma-base, pH 7.4 which was also used throughout the entire slicing procedure.

The slicing procedure was performed by a vibratome (Vibroslicer 752 M, Campden Instruments, Leicestershire, UK) to cut 200 - 300 μ m thick coronal slices which were allowed to recover for at least 45 minutes in Incubation solution at temperature 27-28 °C.

The acute dissociation of the nerve cells was performed by a glass rod (tip diameter of ~ 0.5 mm) mounted on a piezo-electric bimorph crystal, to apply mechanical vibration at sites on slices composed mainly of grey matter²⁴. Dissociated cells were then inserted to a gravity fed perfusion system with very short tubing connected to the anoxic

chamber to reduce mechanical damage to the cells during the loading.

B. Recording solutions

Extracellular solution (EC) containing (in mM) 137 NaCl, 5.0 KCl, 1.0 CaCl₂ ($\times 2H_2O$), 1.2 MgCl₂ ($\times 6H_2O$), 10 HEPES, 10 glucose, 3 μ M glycine, pH 7.4 (NaOH) was used for flushing the cells.

Intracellular solution (IC) containing 140 Cesium-acetate, 3.0 NaCl, 1.2 MgCl₂ ($\times 6H_2O$), 10 HEPES, 10 EGTA, pH 7.2 (CsOH)) was used as pipette-filling solution.

C. Patch-clamp technique

Patch-clamp was used¹ to register the electrical signals across the plasma membrane of single neurons. Electric signal recordings were made between an electrode placed in the outlet of the lab-on-a-chip mounted on an inverted Zeiss Axiovert 25 CFL microscope (Carl Zeiss, Germany) and a recording electrode placed in the micro-pipette that was pulled from borosilicate glass (GC150, Harvard Apparatus Ltd., UK). The recording electrode within the recording pipette was attached to a nerve cell. Pipettes with a resistance of 3-5 M Ω was filled with IC and inserted into the EC-filled micro-channel. Signals were recorded using an Axopatch 200A amplifier, a Digidata 1200 interface and software program pClamp 7 (all from Axon Instruments, Union City, CA, USA). Recordings were made in current clamp and voltage clamp conditions.

D. Oxygen measurement

The oxygen level was controlled with a fiber optic oxygen sensor probe, (FOXY AL300), connected to a Multi-Frequency Phase Fluorometer (Ocean Optics, Dunedin, Florida, USA).

E. Optical tweezers

The optical tweezers were constructed on the inverted optical microscope (Zeiss Axiovert-25 USA) used for patch-clamp, as seen in figure 1. The optical trap consisted of a NIR laser (IQ1A, Power Technology, USA), a 1:5 beam expander and mirrors²³, as shown in figure 1.

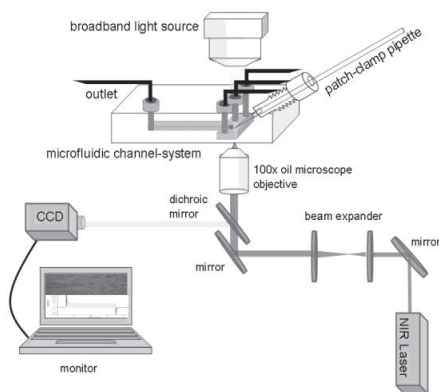


Fig. 1 Schematic figure of the experimental setup including optical tweezers integrated on an inverted microscope.

F. Closed microfluidic system

The PMMA based microfluidic chamber with the integrated patch-clamp pipette was manufactured by CNC; Circuit Board milling technology²³, with micro-channels of 100 μm , sealed by a cover glass using adhesive epoxy. The inlets adjacent to the channels were connected to an external pump system for both the infusion of cells and the solutions with varying oxygen content. The microfluidic chamber was fitted on the microscope, see figure 2.

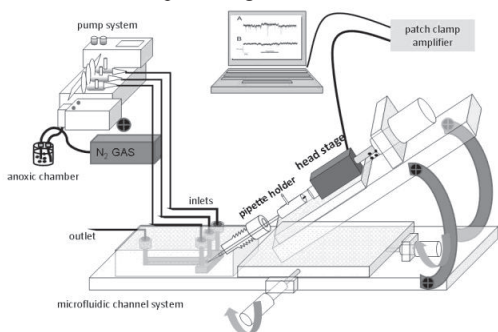


Fig. 2 The microfluidic chamber fitted on the inverted microscope with a lab made head stage holder connected to a pump system.

III. THE EXPERIMENTAL RESULTS AND DISCUSSIONS

First the oxygen content within the lab-on-a-chip was measured with the fiber optic oxygen sensor probe. The normoxic condition was approximately 19-21% O_2 (atmos-

pheric oxygen concentration) while the anoxic conditions were achieved by purging solutions with N_2 gas until an oxygen content of approximately 0.5-1.5% O_2 was achieved. The measurements showed that a reliable control of the oxygen level was established. The time required for the fluid variation within the micro-channel was measured to approximately 3s with a fluid flow rate of 0.1 $\mu\text{l/s}$.

To investigate the impact of the optical tweezers upon the patch-clamp experiments, an optically trapped nerve cell in a Petri dish was steered towards the patch-clamp recording pipette, where it was successfully patched. Application of 12 voltage steps from -74 mV to +46 mV, with a delta level of 10 mV, showed no activation of voltage-gated channels, as can be seen in figure 3A. The voltage-gated channels were not present and no synaptic events could be seen, which indicated that the cell was probably a glial cell. The level of noise seen in the recording did not increase as compared to a previous recording, as seen in figure 3C to 3D. Gap free recordings were made on the cell both in voltage-clamp and current-clamp conditions, as shown in figure 3A, B.

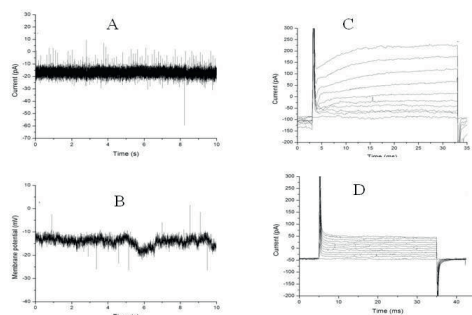


Fig. 3 A) Gap free recordings in voltage-clamp condition with a holding voltage of -54 mV and B) in current-clamp condition with 0 pA current injected, C) Previous recordings on a neuron without optical tweezers, D) voltage steps from -74 mV to +46 mV (10 mV delta level) applied to patched nerve cell while laser tweezing, figures C and D show no remarkable increase of the noise level.

The results showed that patching a cell by bringing it to the patch-clamp-pipette by means of optical tweezers was feasible. Next, the lab-on-a-chip was tested. The closed microfluidic chamber with the integrated micropipette was placed on the microscope stage and connected to the pump systems for the insertion of cells and for the variation of the oxygenation state of the solution. The micropipette was carefully inserted through the hollow screw into the intersection-zone within the microfluidic channel and monitored visually. The cells were introduced to the microfluidic channel system in a low flow rate (0.1 $\mu\text{l/s}$) to enable the selection of a healthy

cell for experiments. Several nerve cells were brought in contact with the micropipette and seals up to 90 megaohm were achieved. However, the viability of the cells was weak and no gigaohm seal could be reached.

IV. CONCLUSIONS

We have presented a concept to combine a microfluidic system, patch-clamp and optical techniques for single cells investigations under optimal control of the oxygen content. The viability and the transport of the nerve cells within the lab-on-a-chip need further investigations though, before full understanding. Improvements may include shorter transport of the cells with enhanced optimized flow or by modifying the same microfluidic chamber to act as a Petri dish for direct dissociation of the cells within the chamber.

The developed closed microfluidic chamber offered the possibility to analyze individual cells under environmental control with a minimal oxygen-diffusion into the micro-channels. In the future, the system will be refined to perform complete electrophysiological investigations with simultaneous monitoring of the biochemical composition of the sample by optical spectroscopy. The simplicity and stability of the system has excellent potential to enable measurements on the function of NgB upon the electrophysiological functioning of neurons.

ACKNOWLEDGMENT

The authors would like to thank EU Structural fund, Objective 2, Norra Norrland, the Swedish Research Council, and the Kempe Foundation for supporting this work.

REFERENCES

1. Sakmann B, Neher E (1984) Patch-clamp techniques for studying ionic channels in excitable membranes. *Cell*.
2. Park YK, Jung SJ, Yoo J-E, et al. (2003) Effect of acute hypoxia on ATP-sensitive potassium currents in substantia gelatinosa neurons of juvenile rats. *European J physiology*. 446(5):600-606.
3. Hyllienmark L, Brismar T. (1999) Effect of hypoxia on membrane potential and resting conductance in rat hippocampal neurons. *Neuroscience*. 91(2):511-517.
4. Gu XQ, Siemen D, Parvez S, et al. (2007) Hypoxia increases BK channel activity in the inner mitochondrial membrane. *Cell* 131:311-316.
5. Lukyanetz E. (2003) Action of hypoxia on different types of calcium channels in hippocampal neurons. *Biochimica et Biophysica Acta (BBA) - Biomembranes*. 1618(1):33-38.
6. Horn EM, Waldrop TG. (2000) Hypoxic augmentation of fast-inactivating and persistent sodium currents in rat caudal hypothalamic neurons. *Journal of neurophysiology*. 84(5):2572-2581.
7. Wang L, Greenfield LJ. (2009) Post-hypoxic changes in rat cortical neuron GABA A receptor function require L-type voltage-gated calcium channel activation. *Neuropharmacology*. 56(1):198-207.
8. Hamann M, Rossi DJ, Mohr C, Andrade AL and Attwell D. (2005) The electrical response of cerebellar Purkinje neurons to simulated ischaemia. *Brain. Journal of neurology*. 128(10):2408-20.
9. Liu H, Moczydlowski E, Haddad GG. (1999) O2 deprivation inhibits Ca²⁺-activated K⁺ channels via cytosolic factors in mice neocortical neurons. *Journal of Clinical Investigation*. 104(5):577-588.
10. Movafagh S, Morad M. (2010) L-type calcium channel as a cardiac oxygen sensor. *New York*. 1188:153-158.
11. Plant LD. (2002) Hypoxic Depolarization of Cerebellar Granule Neurons by Specific Inhibition of TASK-1. *Stroke*. 33(9):2324-2328.
12. Higashi H, Fujiwara N, Shimoji K and Yoshimura M. (1987) effects of hypoxia on rat hippocampal neurones in vitro. *Journal of Physiology* 131-151.
13. López-Barneo J, López-López JR, Ureña J and González C. (1988) Chemotransduction in the carotid body: K⁺ current modulated by PO₂ in type I chemoreceptor cells. *Science* 241(4865):580-582.
14. Kulik A, Brockhaus J, Pedarzani P and Ballanyi K. (2002) Chemical anoxia activates ATP-sensitive and blocks Ca²⁺-dependent K⁺ channels in rat dorsal vagal neurons in situ. *Neuroscience* 110(3):541-554.
15. Englund M, Hyllienmark L, Brismar T. (2001) Chemical hypoxia in hippocampal pyramidal cells affects membrane potential differentially depending on resting potential. *Neuroscience* 106(1):89-94.
16. Balfour RH, Trapp S. (2007) Ionic currents underlying the response of rat dorsal vagal neurones to hypoglycaemia and chemical anoxia. *Journal of physiology* 579(3):691-702.
17. Zaharchuk G, Martin AJ, Rosenthal G, Manley GT, Dillon WP. (2005) Measurement of cerebrospinal fluid oxygen partial pressure in humans using MRI. *Magnetic resonance in medicine. J Society of Magnetic Resonance in Medicine* 54(1):113-121.
18. Schütze K, Pösl H, and Lahr G. (1998) Laser micromanipulation systems as universal tools in cellular and molecular biology and in medicine. *Cell. Mol. Biol.* 44(5):735-746.
19. Yao L, Liu B, Chen T, S. Liu, and Zuo T. (2005) Micro flow-through PCR in a PMMA chip fabricated by KrF excimer laser. *Biomed. Microdevices* 7(3):253-257.
20. Madou MJ. (2002) Fundamentals of Microfabrication: The Science of Miniaturization. 2nd ed. (CRC Press).
21. Ramser K and Hanstorp D. (2010) Optical manipulation for single-cell studies. *J Biophotonics* 3(4):187-206.
22. Ashkin A, Dziedzic JM, and Yamane T. (1987) Optical trapping and manipulation of single cells using infrared laser beams. *Nature* 330:769-771.
23. Alrifaiy A and Ramser K. (2011) How to integrate a micropipette into a closed microfluidic system: absorption spectra of an optically trapped erythrocyte. *J biomedical optics express* 2(8):2299-2306.
24. Vorobjev V. (1991) Vibrodissociation of sliced mammalian nervous tissue. *Journal of Neuroscience Methods* 38(2-3):145-150.

Authors: Ahmed Alrifaiy, Nazanin Bitaraf
Institute: Computer Science, Electrical and Space Engineering
Street: Luleå University of Technology
City: Luleå
Country: Sweden
Email: ahmed.alrifaiy@ltu.se, nazanin.bitaraf@ltu.se